

**ALMA MATER STUDIORUM - UNIVERSITÀ DI BOLOGNA
CAMPUS DI CESENA**

**DEPARTMENT OF ELECTRICAL
AND INFORMATION ENGINEERING
"GUGLIELMO MARCONI"**

SECOND CYCLE DEGREE IN BIOMEDICAL ENGINEERING

Class: LM-21

**BIOMECHANICAL INVESTIGATION OF
MONOLATERAL EXTERNAL FIXATOR CONFIGURATIONS
DURING BONE LENGTHENING TREATMENT**

Graduation thesis in

MECHANICS OF BIOLOGICAL TISSUES

Supervisor

Chiar.mo Prof. Ing. Luca Cristofolini

Candidate

Alessandra Pernigotti

Co-supervisors

Fabiano Landi

Alan Dovesi

Academic Year 2022/2023

"Inseguì ciò che ami o finirai per amare ciò che trovi"
- Carlo Collodi

Abstract

The topic below concerns the biomechanical investigation of different configurations of the Rekrea, a monolateral external fixator for bone lengthening treatments developed and commercialized by Citieffe s.r.l. The first part of the paper introduces the clinical scenario, the processes that stimulate bone lengthening, the state of the art of these surgical procedures, the different stages into which they are performed and the complications that can occur. In particular, the present work focuses on tibial lengthening thus the geometry of the bone and the related joints at the extremities are described. It emerged how during this treatment it is particularly important to monitor the inter-fragmentary movement between the two stumps, the global displacement between the ankle and the knee joints as well as the stiffness of the entire system. The material and methods used to perform the tests are described: the testing machine, the material used to replace the tibial segment and different thickness bone callus. The assembly details of the fixator are analysed: the frame, the clamps and the bone screws used. Several biomechanical tests are done in order to understand how different configurations of the setup affect the values of the parameters of interest: interfragmentary movement, global displacement and stiffness of the entire system. Different angles of insertion of the bone screws respect to the tibial axis, different thickness of the bone callus placed in the fracture site and different number of bone screws through which the fixator is anchored to the bone are investigated. Data collected from the tests are analysed in order to compute the parameters of interests, to do so appropriate Matlab code was written. Later, statistical tests were done to understand if the configurations in each couple of comparison were statistically different from one another. The limits of each setup were analysed. This data will be available for other researches. Finally, the conclusions reveal the salient features of the comparisons between the different configurations; it is also pointed out which ones are efficient in terms of performance and are in agreement with the parameter values reported in the literature.

Contents

1	Introduction	9
1.1	Clinical Scenario	9
1.1.1	Bone growth stimulation	10
1.2	Bone lightening	12
1.2.1	Surgical treatment evolution	13
1.2.2	Treatment phases	15
1.2.3	Treatment studies	18
1.3	Tibial lengthening treatment	23
1.4	Interfragmentary movement, global displacement and stiffness	26
1.5	Objective of the thesis	29
2	Materials and Methods	30
2.1	Experimental Setup	30
2.1.1	Simulated Bone Callus	32
2.2	Rekrea Fixator Components	33
2.2.1	Frame	33
2.2.2	Clamps	34
2.2.3	Bone screws	36
2.3	Mechanical tests	37
2.3.1	Lock/Unlock configuration testing	37
2.3.2	Simulated bone callus validation testing	38
2.3.3	Rekrea Tandem Assembly configurations mechanical testing	39
2.4	Data analysis	42
3	Results and discussions	45
3.1	Lock/Unlock configuration outcomes	45
3.1.1	Results	45
3.1.2	Statistical results	46
3.1.3	Discussions	46
3.2	Simulated bone callus outcomes	48
3.2.1	Results	48
3.2.2	Statistical results	48

3.2.3	Discussions	49
3.3	Rekrea Tandem configuration outcomes	51
3.3.1	Results for the MedioLateral application of the fixator . .	51
3.3.2	Results from the AnteroPosterior application of the fixator	56
3.3.3	Statistical results	62
3.3.4	Discussions	63
4	Conclusions	67
	List of Figures	70
	List of Tables	73
	Bibliography	74
	Acknowledgements	78

Chapter 1

Introduction

1.1 Clinical Scenario

The musculoskeletal system is the system responsible for movement and stability. It consists primarily of bones, muscles and joints. Bones provide structural support, protect organs, and are involved in the production of blood cells. Muscles, through contraction, generate movement, while joints allow for the flexibility and mobility of the bones. Bones can break due to trauma, falls, or excessive strain.

Worldwide, the 85% of extreme limb injuries comes from lower limb cases. Lower limb region includes femur, patella, tibia, fibula, talus, hind foot, mid-foot and forefoot bone. Fractures of the lower limbs are the most common large-organ traumatic injuries to humans [1].

A bone may be completely fractured or partially fractured in any number of ways.

Fractures can be: stable - if the shattered ends of the bone align and hardly move from their original positions; open - if the bone punctures the skin and the wound exposes the bone; transverse - if the bone has a horizontal fracture line; oblique - if the fracture has an angled pattern and shattered - if more piece of the fractured bone are present.

The tibia fracture is the most common; it contributes to at least 8.1% to 37% of lower limb injuries per year. Tibial injuries can be caused by an excessive internal force (compression, torsion, and shear) at the knee and/or ankle joint. Depending on the fracture types, the treatment can be: cast immobilization, functional cast, traction, internal or external fixation. In this last type of treatment the doctor places screws into the broken bone above and below the fracture site; the bone screws are connected to a frame outside the body that stabilizes and holds the bones. When a fracture is complex or does not heal properly, surgical intervention may be necessary.

This intervention entails an osteotomy, which is a procedure in which the bone

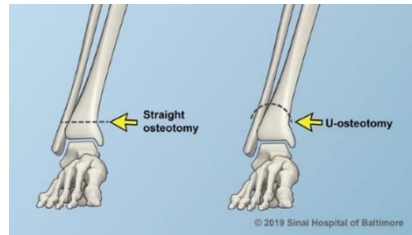


FIGURE 1.1: Shape of the osteotomy, reproduced by [3].

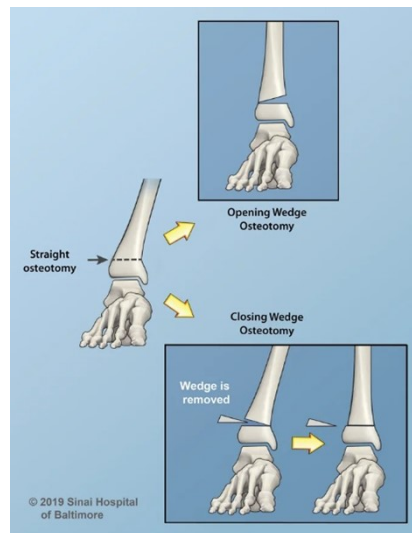


FIGURE 1.2: Types of osteotomy, reproduced by [3].

is surgically cut and realigned. The objective of the osteotomy is to interrupt the bone continuity so that the optimum local conditions for callus osteogenic proliferation are obtained [2]. While fractures are accidental bone injuries, osteotomies are planned surgical procedures that involve manipulation of the bone to enhance its shape or function. Osteotomies can be differentiated depending on their shape: straight, curved and U-shaped (Figure 1.1). In particular, the first one, can be either an open wedge or a closed wedge (Figure 1.2). The choice of the type and the shape depends on the specific treatment needs. Since the bone has the ability to regenerate itself, it may be lengthened, straightened, or shortened during the surgery or gradually after the surgery [3]; therefore, after the osteotomy, the surgeon may apply an external fixator with post-surgery adjustments of the device. To ensure an adequate bone callus mechanical stimulation, in terms of loads applied, it is important to take into account the mechanical behaviour of the external fixator assembly.

1.1.1 Bone growth stimulation

Long bones have a central part, called diaphysis, and two ends known as epiphysis; the latter, covered with cartilage, form the articular surfaces (Figure 1.3). The long bones are thinner in the centre and their diameter increases as we move from the diaphysis towards the epiphyses: this area between one

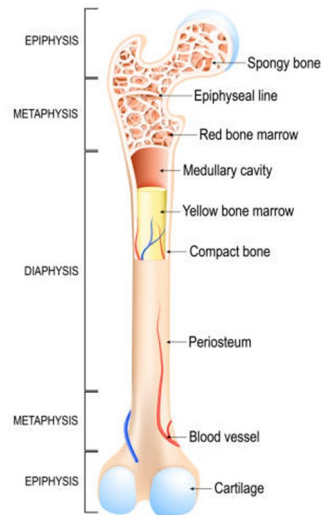


FIGURE 1.3: Structure of a long bone, reproduced from [4].

end of the diaphysis and the adjacent epiphysis is known as the metaphysis. In children and adolescents, between the metaphysis and the epiphysis there is cartilage, which represents the area of growth in length of this type of bone. In adults, the metaphysis is completely ossified. The surface of long bones is covered by the periosteum, a connective membrane responsible for the bone growth processes and the formation of calluses in case of fractures. Compact bone is composed of a series of osteons that are the structural units. At the centre of each osteon is the Haversian canal, which contains one or more blood vessels responsible for vascularizing the structure and eliminating waste substances. Cortical bone serves as the outer shell of the bone. Below the compact bone lies the trabecular or spongy bone. This bone consists of trabeculae, which make the bone highly porous. The main functions of the tissue are to reduce the overall weight of the bone and to serve as a filler for the compact bone. Within the trabecular bone, bone marrow is contained [5]. Bone tissue is formed and remodelled in response to the mechanical forces it experiences, this mechanism is described by Wolff's law [6] (Figure 1.4).

The formation and adaptation of bone tissue are mediated by bone cells that perceive and respond to local mechanical signals.

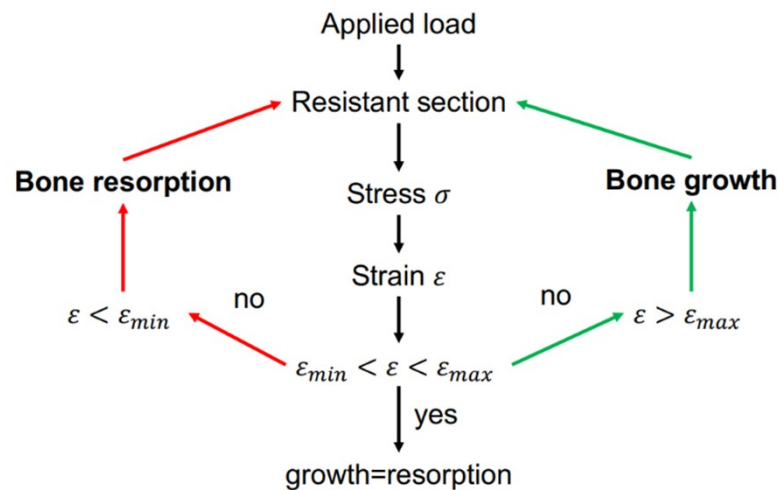


FIGURE 1.4: Wolff' Law.

These are:

- osteoblasts: cells responsible for bone matrix formation;
- osteoclasts: cells responsible for bone matrix disruption;
- osteocytes: cells defined as mechanosensors, able of transform themselves into osteoblasts when subjected to specific stimuli. These cells detect deformations in the extracellular matrix, in which they are immersed, generated by the physical movement of the individual.

Under physiological conditions, our organism maintains a proper balance between the amount of tissue formed and the amount of tissue absorbed, and this prevents the onset of issues.

If bones are subjected to load, that results in a deformation smaller than the physiological value, the process of bone resorption is triggered, which is the reduction of bone mass through the activity of osteoclasts. Conversely, if the amount of deformation experienced by the osteocytes exceeds the physiological value, bone tissue formation is increased. What Wolff's law states is that bone continually adapts to changes in static and dynamic stresses, remodelling itself in a way to consume the minimal amount of bone tissue possible.

1.2 Bone lightening

Controlled lengthening is performed in presence of limb length discrepancy. Relevant discrepancies are considered differences greater than 2 cm. In order to achieve the desired length increase it is advisable to perform the procedure during adolescence. The optimal age to intervene is generally between 7 and 16 years old [2].

Before the surgery, the device configuration and its subsequent implantation

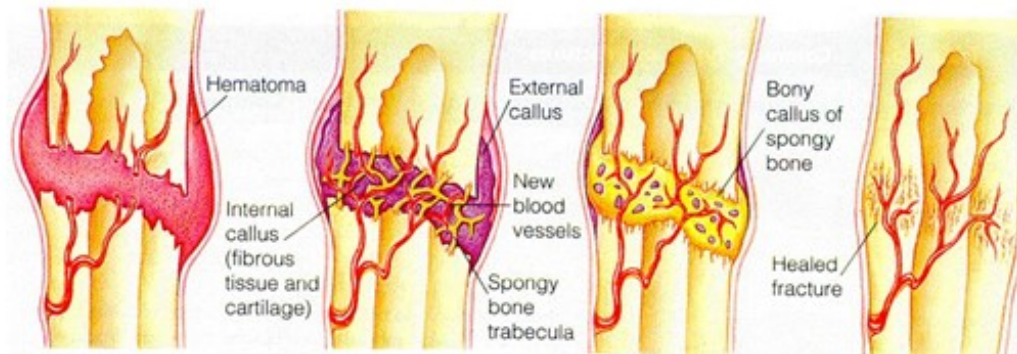


FIGURE 1.5: Callus formation and bone remodelling, adapted from [7].

are chosen, then the osteotomy is performed creating a gap in which callus growth will occur. It is recommended, in clinical practice, to perform the osteotomy in the metaphyseal region, as this area has the highest osteogenic potential of the bone. Following the fracture, blood cells can be observed around the site within a few hours, forming clots or hematomas (Figure 1.5).

1.2.1 Surgical treatment evolution

In the early 20th century, the objective of treatment was bone lengthening without considering the effect on muscle and joints such as the technique continuous extension (A. Codivilla, Bologna, 1904).

This technique described a pin traction plaster that he used to treat patients with coxa-vara, he drove a pin measuring 5 to 6 mm in diameter transversely through the heel, and then with a chisel he made an oblique osteotomy in the middle of the femoral shaft [8].

Main concerns were related to overcome the resistance of the soft tissues without damaging their function and to focus on the response of normal muscle to gradual distraction.

Later, in 1915, Gavril Abramovic Ilizarov developed modular ring fixator (Figure 1.6).

His idea influenced next generations of surgeons and it is still in use.

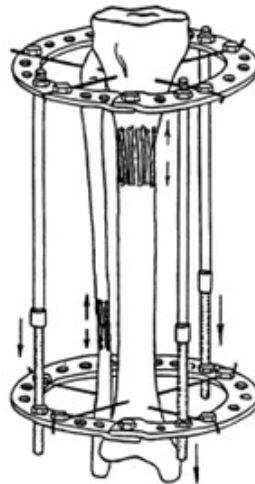


FIGURE 1.6: The Ilizarov ring fixator, 1951, reproduced from [8].

The principles of the Ilizarov fixator are as follows:

- superior quality of the regenerated bone due to the system assembly;
- multistep distraction procedure of 1 mm/day;
- full weightbearing distraction procedure;
- Kirschner wires to fix the two bone segments;
- promotion of healthy joint mobility and tissue nutrition using a device that permits physiotherapy.

Following Ilizarov's lecture in the 1970s, De Bastiani in Verona accepted Ilizarov's concepts and improved them by employing a unilateral dynamizable fixator. One of his innovations completely changed the theory and method of callostasis, or callus distraction: following an osteotomy, he waited 14 days before beginning distraction, allowing for the growth of new callus.

Unilateral external fixation frames differ from circular frames (Figure 1.7) since the first are positioned on one side of the limb, they allow easier insertion and are generally better tolerated by patients due to the reduced bulk of the structure.

External fixation devices are used for the treatment of various pathologies, and one of the most critical aspects of its use is the choice of the configuration, which depends not only on the device itself but also on the patient being treated.



FIGURE 1.7: From left to right: external fixator with circular and unilateral frame, adapted from [9] and [10].

In addition, the external fixators compared to the internal plates and the intramedullary nails are less invasive, ideal for managing soft tissues, allow post-operative adjustment during bone lengthening and manipulation of fragments in case of bone fracture. These are the reasons why in recent decades external fixation has become one of the main techniques used for the treatment of numerous bone tissue pathologies.

This work focused the attention on the application of an external fixator named *Rekrea* made by the company *Citiefte srl*, Bologna.

It is indicated in adult or pediatric patients in reconstructive procedures for the treatment of shortening and lengthening of upper and lower limb, bone loss and deformity correction.

1.2.2 Treatment phases

The treatment of monofocal controlled bone lengthening after the osteotomy can be divided into four different phases, as described below, followed by the removal of the fixator [2].

Latency Phase: after surgery a hematoma begins to form in the osteotomy gap, then the periosteal membrane near the osteotomy starts to promote the activity of chondroblasts, which are responsible for the formation of hyaline cartilage. Periosteal cells at the extremities of the fracture gap are transformed into osteoblasts and begin to form bone tissue that tends to bridge across to the tissue on the other side of the cut.

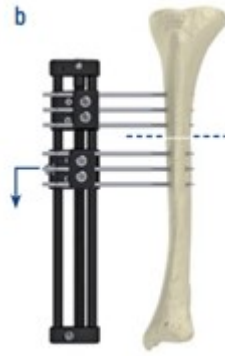


FIGURE 1.8: Distraction phase, reproduced from [10].

This phase has two objectives:

- facilitate the healing of surgical wounds;
- facilitate cell proliferation by forming a bridge between the two bone segments so that they can stabilize.

The duration of this phase (7-10 days) varies depending on the age of the patient, the type of disease and many other factors that are related with the osteogenic capacity of the bone. This is higher if adequate vascularization is present.

Distraction Phase: if radiographic checks reveal that the callus begins to form, the distraction or lengthening phase starts (Figure 1.8). The patient, by rotating a T-shaped key inserted into the proximal or distal terminal of the external fixation frame, achieves incremental distraction of a few millimetres with each click of rotation. When using the Rekrea device, increments of 0.25 mm are performed every 6 hours in order to reach a lengthening of 1 mm per day, unless complications arise.

The separated bone segment is gradually moved using a transport system that applies continuous traction and corresponding stretching to the healing area. Additional fibroblasts proliferate in the callus, depositing collagen, which is organized into fibrils in the direction of distraction.

This results in the development of a fibrous zone containing highly proliferative cells. The first radiographic check is one week after the start of this phase of the treatment, while the subsequent ones are one month apart.

If there is pain, muscle spasms or from the X-ray-images are present signs of poor callus formation, the distraction rate is reduced. Contrarily, if there is excessive ossification with the risk of premature consolidation, the lengthening rate is increased [2].

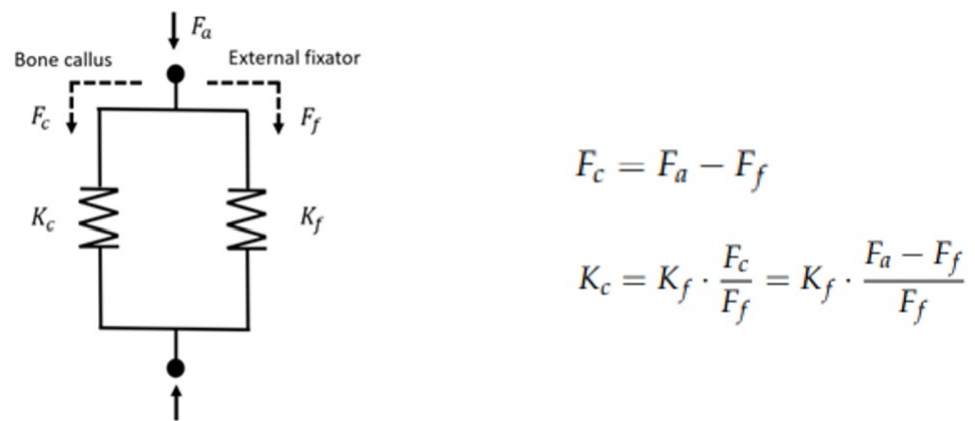


FIGURE 1.9: Mechanical scheme of the system composed by the treated bone and the fixator, adapted from [11].

Neutralization Phase: once the desired length is reached, the fixator is locked to stabilize the bone regeneration; it is appropriate to subject the treated limb to a load sufficient to allow the maturation of the bone callus [2].

Dynamization Phase: once the callus is mature, the fixator is placed in dynamic mode so an axial load is gradually transferred from the fixator to the bone callus in a way proportional to the stiffness of the fixator (Figure 1.9) [2].

Where:

- F_a overall force acting on the structure,
- F_c force through the bone callus;
- F_f force through the fixator;
- K_c stiffness of the bone callus;
- K_f stiffness of the fixator.

At the beginning of this phase the load is completely on the fixator while at the end it is completely on the callus (Figure 1.10). The dynamization increases bone thickness preventing fracture or non union after removing the fixator body. A critical aspect of that phase is the stiffness of the fixator - a rigid system causes delays in bone consolidation, while a certain level of mobility obstructs callus formation. Controlled axial load improves bone healing but movement of the bone in other planes causes shearing and bending forces that inhibit bone formation; therefore a good fixator should be able to control these.

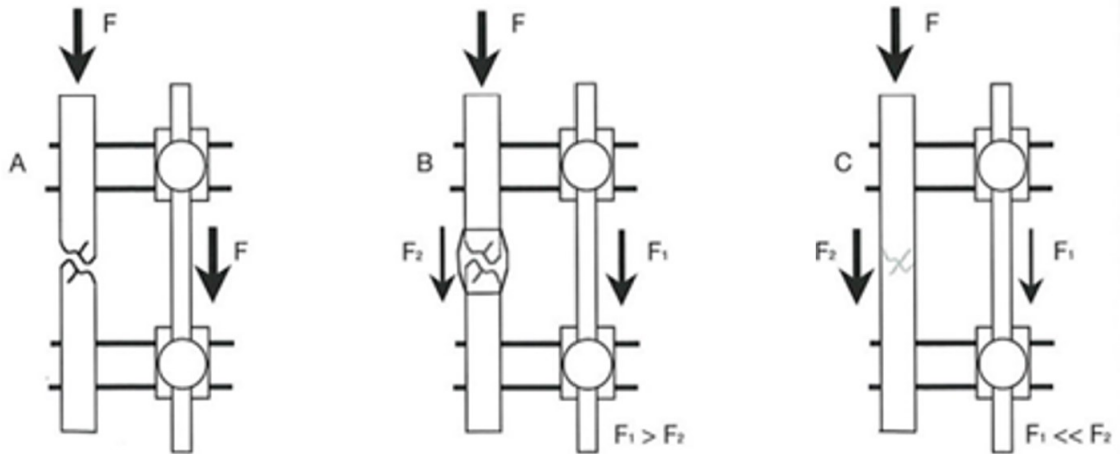


FIGURE 1.10: Transformation of the bone callus during dynamization phase, adapted from [11].

Once this final dynamization phase is completed, and proper bone maturation is achieved, the fixator is removed; it is important to leave the bone screws in place for 3 or 4 days to have the possibility of repositioning the fixator in case of length loss or complications.

Before removing all the components the callus rigidity is checked through radiography; despite these, re-fracture can occur in 3 to 10% of cases.

According to more precise research, when we obtain a stiffness of 15 Nm/degree in the sagittal plane, the consolidation of the tibial fractures is appropriate for the removal of the fixator [12]. Sometimes, after the removal of the fixator, it could be useful to support the bone with other immobilization methods for 2 or 3 weeks to ensure a better bone consolidation.

1.2.3 Treatment studies

Due to their duration, complications might arise during the treatment.

A parameter that can be considered to evaluate the length of the treatment is the healing rate, this is calculated by dividing the total treatment time (in days) by the elongation achieved (in cm); therefore it indicates the number of days of treatment required for the consolidation of a centimetre in an elongation [2]. During the monofocal controlled lengthening technique, the axial distraction force, applied by the fixator, must be greater than the resistance imposed by the formed bone callus and the surrounding soft tissues. The total distraction force will, therefore, be composed of the force required to distract the callus tissue in the osteotomy gap, as well as the force needed to overcome the resistance of soft tissues, such as muscles [13]. The latter, in addition to undergoing elongation during the treatment to which they resist, are also severed by the progressive movement of the fixator's bone screws.

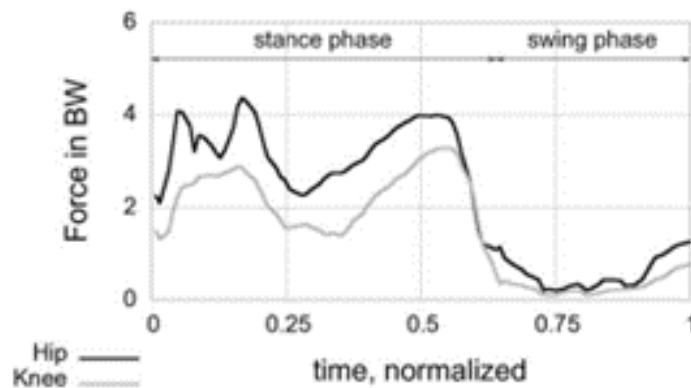


FIGURE 1.11: Resultant hip contact force and knee contact force, both in BW, reproduced from [14].

To understand the force and internal moments, authors simulated the cutting plane at nine different locations [14]. The models that authors used to estimate the internal loads was driven by the gait analysis dataset "man": the shank was considered a rigid body, on it optical markers were placed and ground reaction force was measured with two Kistler plates. The cutting plane was always perpendicular to the longitudinal axis of the tibia, with the distance L_d to the ankle joint. The AnyBody program estimated the muscle forces to meet the rigid body system's balance requirements in each simulated gait time step. The highest internal loads corresponded to the axial force and the bending moment in the sagittal plane. The late stance phase was the one in which the tibia experienced its greatest internal force, which always operated in the longitudinal direction (Figure 1.11). However increasing the osteotomy distance from the ankle joint, the moments in the sagittal plane increased up (Figure 1.12). In the study reported [15], axial forces were measured during various bone lengthening treatments. Specifically, in each monolateral external fixation device, a load cell was incorporated to measure the axial distraction force before and after each lengthening increment. The distraction increments were measured using the calibrated wire on the fixation device body.

The trend of the total distraction force over time during the lengthening phase was characterized by peak forces and resting forces (Figure 1.13). When a roughly constant force level was reached, the remaining force is defined as the resting force (Figure 1.14). After each distraction increment, there was an instantaneous increase in the force value until the peak value was reached.

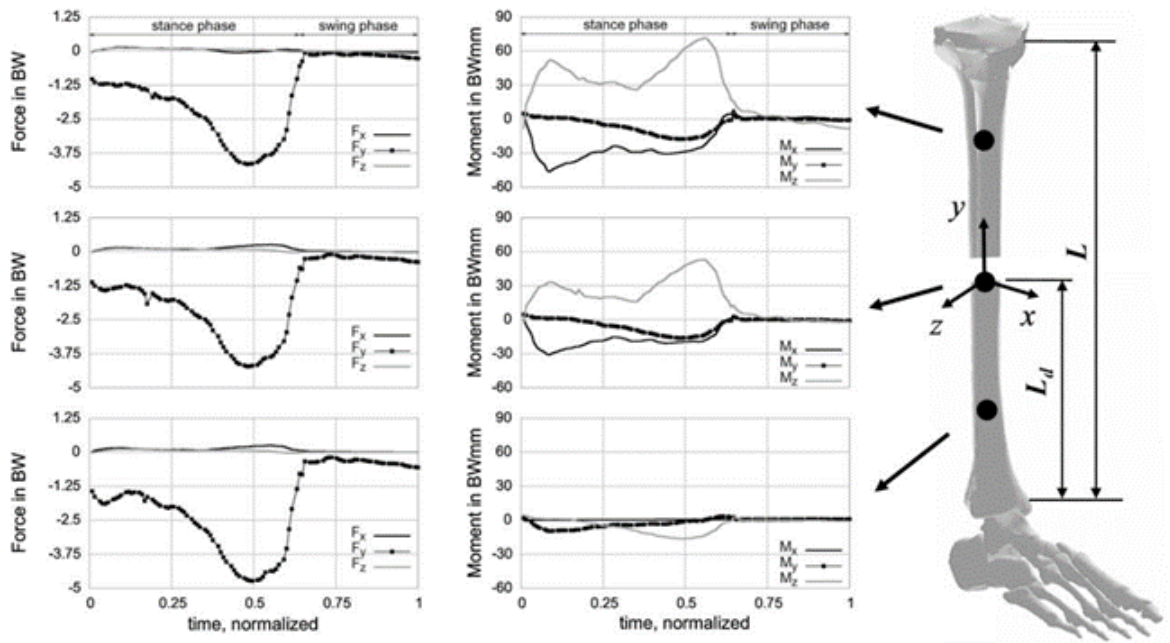


FIGURE 1.12: Internal forces in BW (left) and internal moments in BWmm (right) over the gait cycle at the three locations along the tibial axis, reproduced from [14].

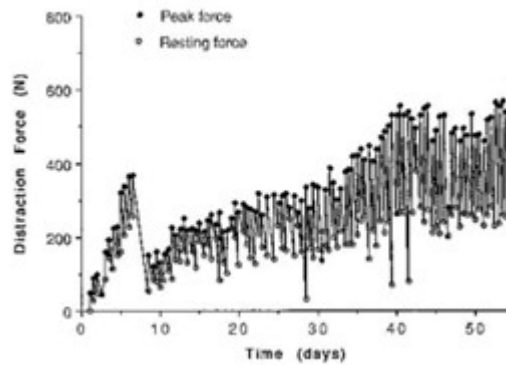


FIGURE 1.13: Distraction force in time in a tibial lengthening treatment, reproduced from [14].

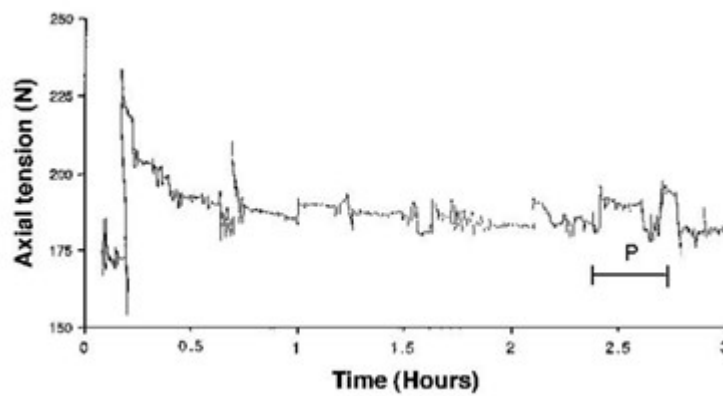


FIGURE 1.14: Force readings after a lengthening of 0.25 mm, reproduced from [14].

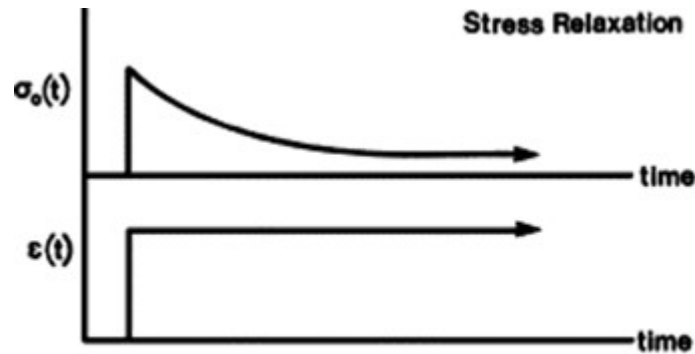


FIGURE 1.15: Viscoelastic behaviour of soft tissue, adapted from [16].

The peak force decreased exponentially after each lengthening increment due to the viscoelastic behaviour of the tissues (Figure 1.15), characterized by stress relaxation, which involved a decrease in stress over time while the imposed deformation remains constant.

Authors [14] [15] [17] [18] have reported axial forces registered during distraction phase while treating of tibial lengthening, and it was possible to sum up that the range in which were the forces during the treatment is: 250 N - 1000 N. This range of magnitude was so wide because the values of those forces depended on the location of the cutting plane, the phase of the motion, the task that perform the subjects, the velocity of walking and the type of pathology that was treated.

Same consideration could be done for the moments that were much larger in the medio/lateral axis.

Therefore, to proper planning and execute the treatment, it is necessary to analyse in detail the patient's characteristics. A first subdivision is possible by dividing the treated patients in two categories:

- patients with post-traumatic shortening: following trauma or a medical condition, some patients exhibit a difference in limb length;
- patients with congenitally short limbs: they exhibit a difference in limb length from birth.

From scientific literature it has been possible to define that subjects with congenital discrepancies exhibit, during the lengthening phase, forces of greater magnitude compared to the post-traumatic one (Figure 1.16).

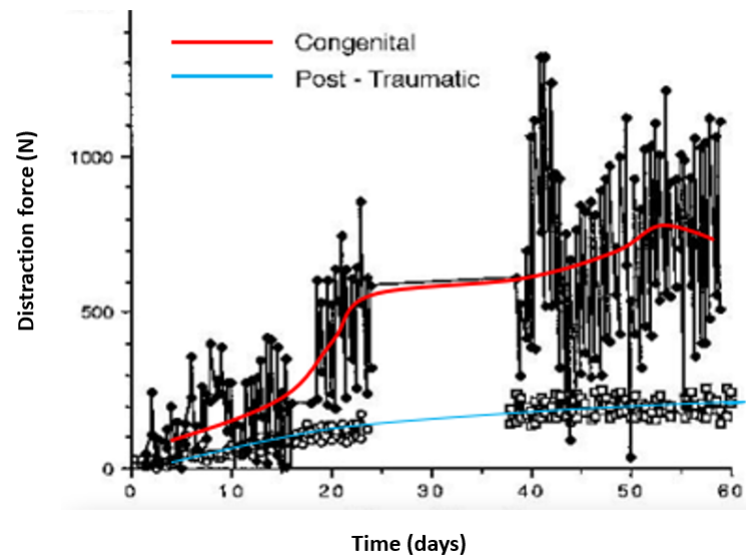


FIGURE 1.16: Distraction force in case of congenitally short limbs (red line) and traumatic shortening (blue line), adapted from [14].

This result was correlated with the fact that the limb length discrepancy present from birth also affects the length of the soft tissues, which will therefore be shorter than in a physiological condition. Therefore, with each increment of distraction, the soft tissues had to adapt to reach lengths never reached before. This did not happen in patients who had been in an incident because the treatment was performed following trauma or the onset of a medical condition, both of which generate limb length discrepancy. In these last patients, since the length of the soft tissues corresponded to the physiological condition, the reduction in limb size led to the loosening of the surrounding soft tissues, which, after the distraction increment, tended to generate lower resistance forces.

In addition, patient with congenitally short limbs developed not only high peak forces but also a large amount of relaxation; in those cases muscles and soft tissues reacted unfavourably to distraction when the limb length was increased of more than 10%.

Nevertheless, since several radiographs were taken in the weeks during lengthening, complications such as valgus deformity of the tibia or deformity of the joints adjacent to the treated segments were noted. When high forces developed, distraction was stopped temporarily because if during lengthening phase the axial forces exceeded the levels that the fixator could, this caused the failure of the frame or damage to the cartilage in the adjacent joints.

These forces caused by muscles and tendons attached to the bones could not be suppressed by the patients, even if they tried to prevent the overload of the treated leg they could not suppress the muscle contractions when they walked with crutches.

During tibial elongation procedure the tension generated on the gastrocnemius caused the equinus deformity and less frequent also the joint subluxation. To prevent musculotendinous contraction the soft tissues could be released during the surgery and active physiotherapy was done throughout the treatment. Then the muscle tension during the neutralization phase began to decline allowing the joint movement.

Since this lengthening procedure had a long duration in time, the patients had to be informed about the cleaning of insertion sites, to prevent infections and how to perform the distraction [19]. The use of hydroxyapatite-coated bone screws could significantly reduce the incidence of infection at the screw insertion site, thanks to a greater capacity for osseointegration with the bone.

1.3 Tibial lengthening treatment

As cited before one of the possible complications that could happen during bone lengthening was the joint subluxation that happens when a load is applied to an unstable joint; therefore the partial loss of normal anatomical relationships between the joint surfaces happens.

The bones involved in joints are characterized by a mechanical axis and an anatomical axis (Figure 1.17); these are two concept used to describe the structure and the orientation of the bone itself.

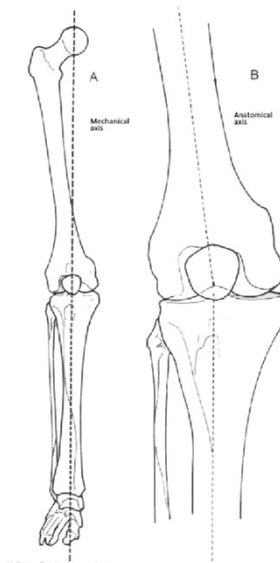


FIGURE 1.17: Mechanical (A) and anatomical (B) axis of the entire leg, adapted from [20].

The anatomical axis of a bone is an imaginary line that represents the direction of its length. This axis generally coincides with the midshaft line, which is the central or median point of the bone. The anatomical axis is important for describing the overall orientation of the bone within the body.

The mechanical axis of a bone is a concept related to the forces and movements that the bone can withstand and generate. This axis connects the proximal and distal joint centres, it represents the direction along which biomechanical forces act on the bone and it is used to assess the function of the bone in situations such as loading and joint movement. The mechanical axis is significant in biomechanics and orthopedics to understand how bones respond to mechanical stresses.

In particular, in the case of femur treatment, performing lengthening along the anatomical axis forces the mechanical axis of the joint in a lateral direction, causing a valgus deformity of the knee. It should be considered that positioning the body of the fixator parallel to the mechanical axis results in a higher tensional state at the screw-bone interface since the screws will not be inserted perpendicularly to the bone itself [2]. This considerations do not regard the tibia because in this bone the anatomical axis coincides with the mechanical one therefore, for the treatments of the tibia there is no doubt if the fixator has to be aligned with the anatomical axis or with the mechanical one. In literature it is reported that for tibial lengthening the mediolateral positioning of the fixator gives high stability but it can be uncomfortable for the patient to walk, therefore, usually surgeons opt for anteromedial application that guarantees enough stability and comfort for the subject. Other authors, suggest that to avoid valgus deformities it is recommended the anterior positioning of the fixator.

The first screw of the setup that is implanted is the proximal one followed by the most distal of the frame and consequently the remaining screws.

Depending of the height on which the screws are inserted in the tibia, attention should be paid to soft tissues and blood vessels that may be encountered. For example in the proximal part of the tibial tuberosity the anterior zone on both sides of the patellar ligament is safe for unilateral fixation (Figure 1.18). While distal to the tibial tuberosity it is best to insert the pins where soft-tissue coverage is minimal so the risk of pin track infection is lower (Figure 1.19).

In the middle part of the tibia near the posterolateral tibial border runs the neurovascular bundle that includes the deep peroneal nerve, anterior tibial artery and vein therefore if the screws are inserted as shown by the red dotted line, they could be dangerous [21] (Figure 1.20). Also the distal zone of the tibia (Figure 1.21) is critical for the screws insertion because the peroneal nerve, the anterior tibial artery and vein are very close to the posterolateral bord of the tibia; therefore, in literature precise guidelines for the surgeons regarding the insertion of the screws are reported.

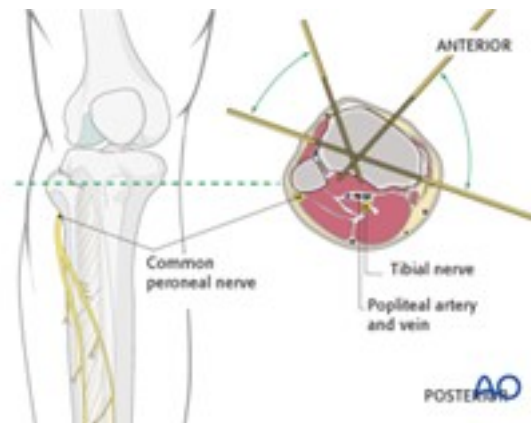


FIGURE 1.18: Screw insertion in the proximal part of the tibia, reproduced from [21].

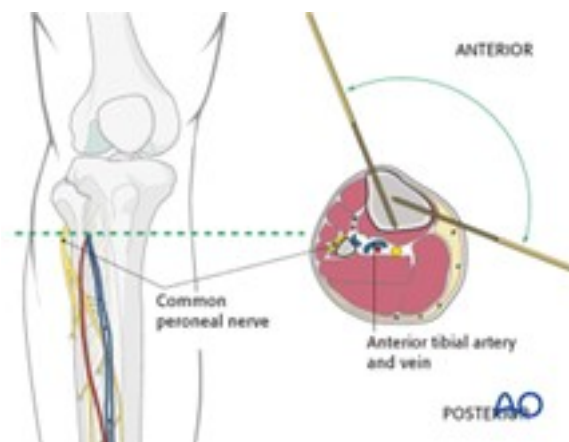


FIGURE 1.19: Screw insertion in the distal part of the tibia, reproduced from [21].

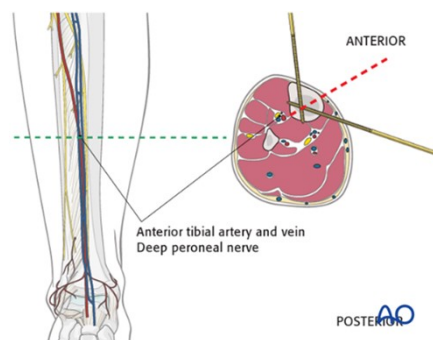


FIGURE 1.20: Screw insertion in the middle zone of the tibia, reproduced from [21].

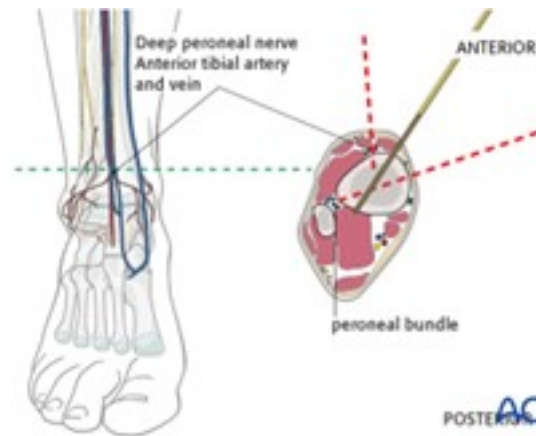


FIGURE 1.21: Screw insertion in the distal zone of the tibia, reproduced from [21].

1.4 Interfragmentary movement, global displacement and stiffness

There are numerous strategies to get a tibia fracture to heal. One of them is that the external fixator used to repair the fracture should be as stable as possible because this speeds up the healing process. According to the authors [22], when compared to internal fixation methods (screws, plates, and wires) the external fixation is the most stable fixation. The stability of the fixator can alter the healing rate. The use of external fixator, through the screws and the frame, is the favourable option to allow weight bearing forces to be distributed from the upper to lower patient's body.

A fundamental aspect of the entire external fixation system during bone lengthening is the axial stiffness, it primarily depends on the configuration of the device chosen for the specific treatment which is characterized by various factors, including:

- the number of bone screws: the more screws there are, the greater the stiffness of the construct;
- screw diameter: the larger the diameter of the screws used, the greater the axial stiffness of the construct. However, if the diameter is too large, it can weaken the bone to the point of fracturing it. It is common practice not to use a screw diameter greater than one-third of the diameter of the bone in which it is fixed [2];
- clamp-to-first cortical distance: the smaller the clamp-to-first cortical distance, the greater the axial stiffness of the construct. This distance is, in fact, nothing more than the lever arm of the force acting on the bone to be treated, and as it increases, the bending moment to which the bone screws are subjected also increases [23].

The stiffness of the fixator depends on the phase of the treatment. It relates to the strength needed for the device to overcome the peak pressures, caused by

the stretching resistance imposed by soft tissues, and the resistance created by the bone callus during the distraction phase. The amount of axial stiffness during consolidation is associated with the interfragmentary movements required to facilitate the mineralization of the bone callus in the fracture gap.

Two characteristics of the construct are therefore important: stability and deformability.

The stability of the system is a crucial factor for a successful treatment outcome, it refers to the ability of the device to withstand the loads it is subjected without permanent changes in the configuration of individual components. The most important factors influencing the stability of a fixator are the bone-screw connection and screw-frame connection.

The deformability of the construct allows micro-movements at the fracture site, so bone fragments move reciprocally under the influence of applied loads and return to their original position when the load ceases. The deformability of an external fixator can be adjusted by varying the distance between the bars of the frame and the axis of the treated bone, the diameter of the bone screws, their arrangement and number, or their mutual distance.

During the years, the clinical opinion of ensuring a configuration with the highest possible axial stiffness, has given way to the need to promote micro-movements to the bone callus, thanks to the elasticity of the construct. A mechanically stable fixator determines the interfragmentary movement in the fractured area where the callus forms during the healing process, allowing the bridging of the fracture gap [24].

Therefore, it is clear that the movements between the fracture surfaces are essential during the healing process, even if the most beneficial environment for the healing of a fracture is not fully explained [25]. Having high stress and strain at the pin bone interface may create the risk of pin loosening and infection. An excessive movement in the fracture gap is undesirable for the healing process and may increase the risk of pseudoarthrosis. From the analysis of the articles available in the scientific literature, it has emerged that: movements in the fracture gap ranged between 0.1 – 1.3 mm in axial direction and 0.2 – 0.5 in shear direction are known to be beneficial, but if they are greater than 2.0 mm they could lead to complications and if they are lower than 0.1 they may cause bone resorption (Figure 1.22) [24] [25] [26] [27].

The evaluation of these value ranges is currently under investigation. In general, the frames should be quite steady at first, in order to promote fracture healing; then the frames must be increasingly dynamized as the healing continues. In this stage, the osteogenesis site gradually receives an increasing strain. As there isn't a widely used method, the dynamization of the fixator can either be done by extending the space between the frame and the bone or by removing part of the bone screws.

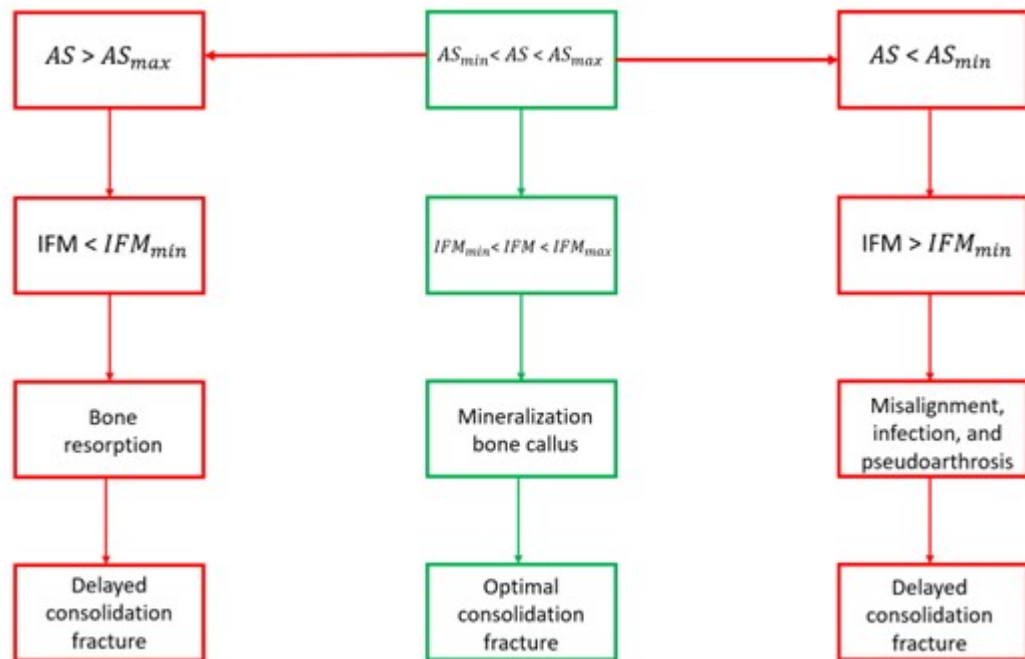


FIGURE 1.22: Axial stiffness (AS) and interfragmentary movements (IFM) relation.

In this work for each configurations are evaluated the interfragmentary movements and also the global displacements that indicate how close the ankle joint approaches the knee, this last index reflects in the global stiffness of the construct. This indexes are monitored during all the healing process till the removal of the fixator before which radiographic examination are done to evaluate the consolidation of regenerated tissue, this images only offer quantitative data that are unrelated to the mechanical characteristics of the bone. Even after the fixator has been removed, it is usual to keep the bone screws in place for a few days to allow for any required fixator repositioning.

1.5 Objective of the thesis

The literature analysis has revealed how different factors affect the quality of limb lengthening treatment. For this reason, device manufacturers are continuously looking for solutions that provide the best outcome of the treatment, in close collaboration with the medical-scientific environment.

It is necessary to consider how the concepts of stability and stiffness for unilateral external fixation device during the treatment of bone lengthening are critical.

Due to the lack of stiffness of an external fixator system, a cartilaginous callus is more likely to form, it has a harder time turning into bone. As a result, the consolidation process may take longer than expected and pseudoarthrosis may occur. The consolidation of the bone regeneration may be delayed also by excessive stiffness in the later phases of the therapy [2].

In general, a surgeon relies on his or her personal experience to define the best device configuration to use, since no rigorous guidelines that take into account all treatment variables are available. It is also important to remember that during treatment the only way they have to monitor and assess the status of bone callus consolidation are X-ray images.

Citieffe s.r.l. is a company that develops and commercializes surgical instruments for orthopaedic traumatology, particularly implantable devices for internal and external fixation. It is actively engaged in researching the best configuration use of its Rekrea external fixation device based on the patient specifications, through collaborations with users of the device.

In this context, during my curricular internship, I took part in the study of the mechanical behaviour of different configurations during the treatment of tibia lengthening. The fixator was anchored to two tibial bone substitutes, simulating the osteotomy of a real treatment, through a different number of screws, positioned closer or further from the fracture gap. The screws were inserted in a different way in respect to the anatomical/mechanical axis of the tibia, in order to understand how mechanical behaviour changed.

Thickness of the bone callus placed in the osteotomy gap was investigated to understand the effect of this variable.

Data resulting from all the mechanical tests were analysed to evaluate how changing the different configurations brought to a diverse outcomes, which had to meet some basic medical requirements, as described in literature.

The main goals of this thesis were to investigate the performance of the Rekrea device: if it is used in Lock/Unlock configurations, if the thickness of the simulated bone callus is changed and if the number and positioning of pins involved in the Tandem Assembly is changed.

Chapter 2

Materials and Methods

To obtain the results, shown in the following paragraphs, mechanical tests were done.

2.1 Experimental Setup

The tibial bone was simulated with two Teflon (PTFE) cylinders with a diameter of 30 mm and length of 30 cm (similar materials and dimensions respect to bone tissue) separated by a gap that corresponded to the fracture site [28]. The external fixation device was anchored to the simulated bones through several bone screws. In the gap between the two bones two "sheaths" were placed to guarantee the uniaxiality of the compression test. Between these, a thin layer of simulated bone callus, obtained from Sawbones block 10 PCF (density of 0.16 g/cm^3) was placed. For the following tests different thickness of simulated bone callus were used, as to simulate a bone growth. On the upper extremity of the construct, the load was applied, through a ball joint or a knee prosthesis. On the lower extremity the structure is supported always by a spherical joint simulating the tibial plafond.

Since the interfragmentary movement plays a key role in the treatment, between the two simulated bones it was necessary to arrange a setup able to evaluate these movements [29]. For this scope an extensometer (model MTS 632.79) was fixed to the structure, at the level of the two "sheaths" that included the bone callus, to measure IFM only in the axial directions without any other interference caused by deformations along other directions. The extensometer (Figure 2.1) was packed in a case which contained: the instrument, the attached cable with connectors, the springs, the attachment devices and the tools.

Testing activities were performed with a universal testing machine: MTS 858 Mini Bionix II Model used in axial configuration (Figure 2.2).



FIGURE 2.1: MTS 632.79 Immersible Extensometer.



FIGURE 2.2: Testing machine.

The analysis of the data from the mechanical tests were obtained using the Matlab R2023a software. From the output data file of the testing machine, the useful columns of data were extracted; then some graphs were obtained such as the load in time (Figure 2.3) in order to see the sinusoidal cyclic load acting on the structure. The last cycle is considered the steady state behaviour of the system therefore it was the one used to compute the parameters of interest, which were:

- IFM: calculated as the difference between the displacement value recorded by the extensometer at the end of the last compression cycle of load and the value of the same variable at the beginning of this cycle;
- DISP: calculated as the difference between the displacement value recorded by the axial LVDT at the end of the last compression cycle of load and the value of the same variable at the beginning of this cycle;
- E_glob: calculated as the slope of the regression line on the curve obtained plotting the load in the last cycle of compression on y axis and the global displacement in the corresponding interval on x axis.

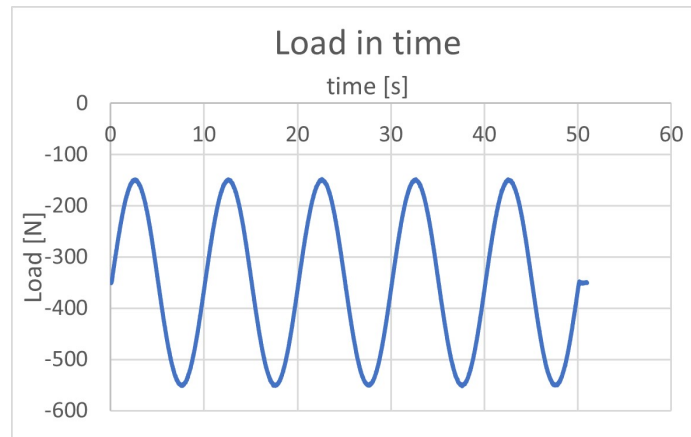


FIGURE 2.3: Load in time acting on the structure.

2.1.1 Simulated Bone Callus

To simulate the bone callus placed in the gap between the two bones segments after the osteotomy a thin layer of Sawbones block 10 PCF (density of 0.16 g/cm^3) was placed.

Sawbones are artificial bones designed to simulate the bone architecture, as well as the bone's physical properties [30]. Plastics and epoxies are the fundamental parts of the sawbones. They are used in applications that previously depended on dead bodies. These applications include orthopedic biomechanics research and surgical teaching. Although cadaveric models are the industry's gold standard simulators, they have significant disadvantages that limit their use in educational facilities. These disadvantages include the risk of disease transmission, high cost, and long preparation times. Furthermore, cadaveric samples represent the elderly people, whose bone quality might not be represent the majority of orthopedic patients.

Sawbones are used by orthopedic educators to demonstrate how soft tissues, such as muscles and ligaments, are attached to bones and how they relate to each other. Additionally, the orthopaedic resident gets the chance to continually practice various orthopedic surgery techniques on sawbones, until a certain level of competence, including fracture reduction, drilling, plate fixation, and screw insertion is reached and without harming patients. The most recent Sawbone generation accurately mimics the biomechanical characteristics of the human bone when subjected to varying loads such as axial, torsional, and bending pressures. They provide exact reconstructions of the anatomical landmarks of the bone with cortical wall thickness that is equivalent to the real bone.

This work demonstrates how the different thickness of the bone callus results in different values of the analysed parameter (IFM and DISP) of the entire construct subjected to axial load.

2.2 Rekrea Fixator Components

Rekrea is a monolateral limb reconstruction system (Citieffe s.r.l.). It has a range of fixator body lengths: Standard, Bifocal and Small. In this last version both the fixator body and the clamps are small.

For this reason, it is recommended for pediatric use.

The main elements of the Rekrea system are:

- Fixator Body;
- Mobile Clamps;
- Bone Screws;
- Kirschner Wire (for the hybrid configuration).

This system meets the requirements of the standard specification and test methods for external skeletal fixation device F1541 -17. This specification is under the jurisdiction of ASTM Committee F04 on Medical and Surgical Materials and Devices.

2.2.1 Frame

The monolateral Rekrea fixator body (Figure 2.4, [10]) is composed of three radiolucent rods: one has the function to move the clamp for the distraction/compression treatment and it is made of a thermoplastic material (Ketron CA30 PEEK), while the other two are made of composite material (carbon fiber).

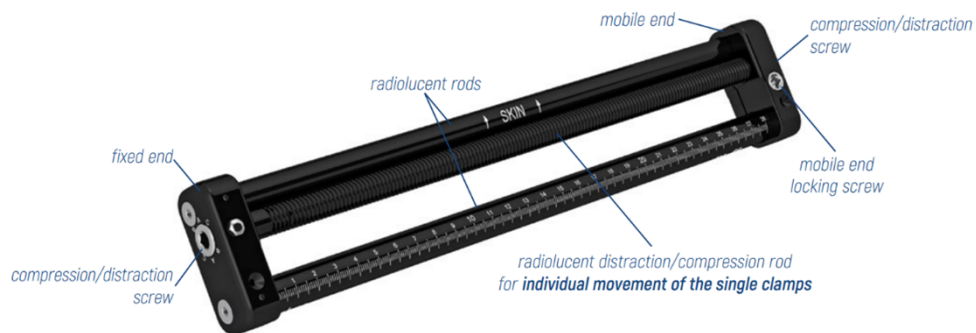


FIGURE 2.4: Monolateral Rekrea fixator body, reproduced from [10].



FIGURE 2.5: Rekrea Small fixator body, reproduced from [10].

The fixator body comes in different lengths and types:

- Rekrea fixator body;
- Rekrea Bifocal fixator body, for treatments involving significant bone transport; it is best to move the clamps in opposite directions or at different speeds;
- Rekrea Small fixator body for small bones.

For the tests performed in this analysis the Rekrea Small fixator body was considered (Figure 2.5).

2.2.2 Clamps

The mobile clamps for bone screws are made in aluminium alloy (7075 Aluminium Alloy - Ergal) and they allow different types of configurations and movements depending on the treatment in which they are involved. The clamps can be used: Straight, Translational, Standard and Swiveling; all the cited types are also available in Small version, to be used with the Rekrea Small fixator body (Figure 2.6).

For the analysis, discussed in the following sections, Standard Small clamps were used. At the base of all Rekrea clamps there are two screws: green "ON" and purple "LOCK-UNLOCK", which control the sliding of the clamp along the fixator body rods (Figure 2.7). When the "ON" screw is tightened, the clamp is locked to the compression/distraction rod; turning the compression/distraction screw moves the clamp. Regarding the "LOCK-UNLOCK" screw, when it is tightened in the "LOCK" position, the clamp is locked. When the screw is loosened in "UNLOCK" position the clamp is free.

For this thesis, mechanical tests were done to understand if significant results emerged when the "LOCK-UNLOCK" and the "ON" screws were in the same position.



FIGURE 2.6: Mobile clamps for Rekrea fixator body and Rekrea Small fixator body, reproduced from [10].



FIGURE 2.7: “ON” and “LOCK-UNLOCK” screws of the clamp, reproduced from [10].



FIGURE 2.8: Steel double-diameter thread bone screw, reproduced from [10].

2.2.3 Bone screws

Bone screws are the elements that, through the clamps, connect the body of the fixator with the treated bone [10]. The Rekrea system uses steel double-diameter thread bone screws (Figure 2.8). These are self-drilling and self-tapping and are designed to achieve optimum capture with minimal damage to the bone tissue. The double-diameter profile is one of the elements that contributes to ensuring the stability of the system. The screws are made of steel 316L that is a non-magnetic material, so that it is not affected by magnetic fields, it has a high elastic modulus and high mechanical properties in compression.

These double-diameter bone screws act as follows:

- the self-drilling tip creates a hole the size of the smallest diameter;
- the smallest diameter inserts into the bone;
- the first self-tapping portion performs the tapping of the bone;
- the second self-tapping portion facilitates the transition to the largest diameter;
- the largest diameter penetrates while correcting any ovalisation of the first hole.

For patients who have inflammatory or allergic reactions to the tip, nickel-free cortical bone screws are available as well as screws covered by hydroxyapatite, due to its high biocompatibility.

Hydroxyapatite is an important mineral component of bones, it is responsible for the consistency and strength. In bones, hydroxyapatite merges with other substances, such as calcium salts and collagen, to form a solid and resilient structure.

Hydroxyapatite is present in bone reconstruction materials to restore and maintain bone structure. It is useful when screws have to remain in place for long treatment.

2.3 Mechanical tests

2.3.1 Lock/Unlock configuration testing

The first tested configuration (Figure 2.9) showed two standard clamps on the Rekrea Small fixator body, the first with three screws and the second with two screws. The first clamp was fixed on the bone segment above the fracture site (proximal clamp), the second on the segment below the gap (distal clamp). Between the two tibial segments a layer of simulated bone callus (Sawbones block 10 PCF) with the thickness of 6 mm and then 9 mm was tested. The joints, so the extremities of the structure were simulated with spherical joints.



FIGURE 2.9: Complete system mounted on the testing machine.

All the system, with the different simulated bone callus thickness, underwent six tests, each test had six repetitions, each repetition composed of 10 load cycles. The sinusoidal load had an amplitude between -150 N and -750N with a frequency of 0.1 Hz. Half of the six tests were executed in UNLOCK configuration, and the others in LOCK configuration.

UNLOCK configuration implies that:

- on the proximal clamp the “ON” screw is loosed while the “LOCK-UNLOCK” screw is tightened;
- on the distal clamp the “LOCK-UNLOCK” screw is loosed while the “ON” screw is tightened.

LOCK configuration entails that on the proximal and distal clamps all the screws are tightened. This setup was not recommended by the company but was investigated to understand how the system (bone-fixator) behaved.

One of the problems in the treatment of the tibia is the deformation that the frame undergoes due to the moment generated by the accumulation of soft tissues present in the posterior area of the tibia [31]. Considering this issue, a particular configuration of the device called Tandem was tested.

2.3.2 Simulated bone callus validation testing

To understand how the simulated bone callus behaves, tests were done without the fixator anchored to the tibial segments (Figure 2.10 and Figure 2.11). Assuming the following period of treatment (6, 10.3, 16.3 and 21.2 mm of bone callus at the osteotomy), the system underwent five compressive tests and for each test five cycles of sinusoidal load were applied, in the range between -150 N and -550 N, with a frequency of 0.1 Hz.



FIGURE 2.10: System without Rekrea anchored mounted on the testing machine.



FIGURE 2.11: Focus on the system without Rekrea.

2.3.3 Rekreia Tandem Assembly configurations mechanical testing

The Tandem configuration shows the distal bone segment connected to two clamps positioned close on the frame of the fixator. In this configuration three clamps are mounted on the frame: on the proximal bone segment; on the distal bone segment, proximally to the osteotomy; and distally on the same bone segment. This configuration allows greater variability in the placement of the bone screws showing the simultaneous movement of both adjacent clamps.

In particular, the configurations that underwent mechanical tests were reported:

- Configuration Tandem central 2screws (Td_central_2screws) (Figure 2.12): three screws were in the proximal clamp, two screws in the clamp proximal to the fracture site (first and last hole of the clamp) and one screw in the central hole of the distal clamp;



FIGURE 2.12: Configuration Td_central_2screws

- Configuration Tandem distal 2 screws (Td_distal_2screws) (Figure 2.13): three screws were in the proximal clamp, one screw in the central hole of the clamp proximal to the fracture site and two screws in the distal clamp (first and last hole of the clamp);

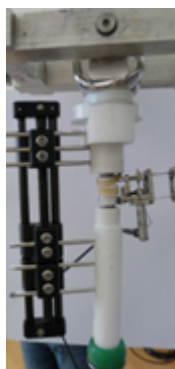


FIGURE 2.13: Configuration Td_distal_2screws.

- Configuration Tandem central full (Td_central_full) (Figure 2.14): three screws were in the proximal clamp, three screws in the clamp proximal to the fracture site and one screw in the central hole of the distal clamp;

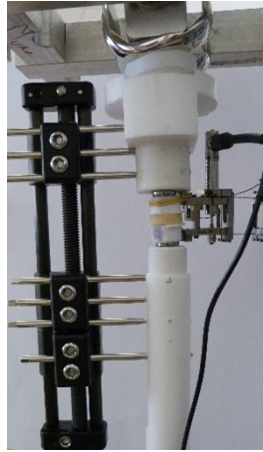


FIGURE 2.14: Configuration Td_central_full.

- Configuration Tandem distal full (Td_distal_full) (Figure 2.15): three screws were in the proximal clamp, one screw in the central hole of the clamp proximal to the fracture site and three screws in the distal clamp;

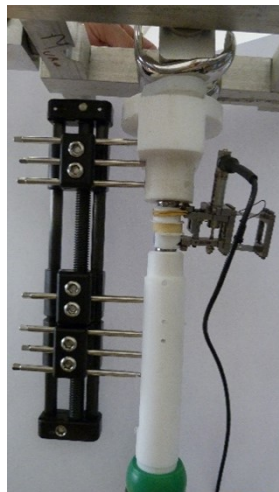


FIGURE 2.15: Configuration Td_distal_full.

For all the systems cited, both for 6 mm and 9 mm of simulated bone callus, five tests of cyclic load were executed in LOCK configuration and 5 cycles in the UNLOCK configuration. The sinusoidal load had an amplitude between -150 N and -550N with a frequency of 0.1 Hz. These tests were executed when the fixator was positioned in the mediolateral direction (ML, 45°) in respect to the tibia and also in the anteroposterior direction (AP, 0°) respect to the tibia (Figure 2.16 and Figure 2.17).

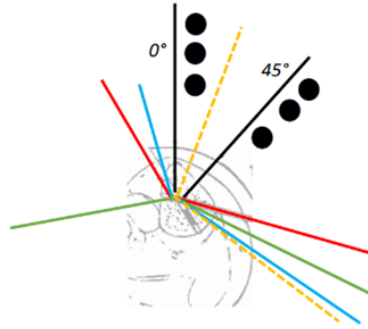


FIGURE 2.16: Directions of the insertion of the screws in the bone, adapted from [21].

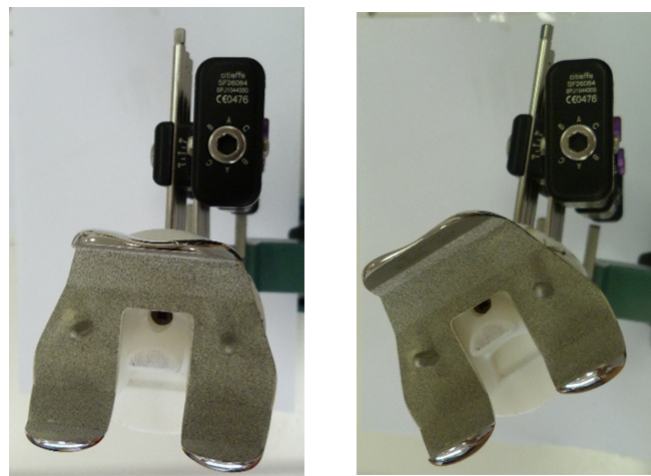


FIGURE 2.17: Anteroposterior and mediolateral positioning of the fixator.

The ML application is the most commonly used during surgical procedure, but for the purpose of this research the AP application was tested; the moments were analysed to investigate the effect of maximizing the angle of pin insertion.

The comparison of the results obtained in all the different configurations reported above are explained in detail in the dedicated section (Paragraph Results and Discussion).

2.4 Data analysis

The data obtained from the mechanical tests were compared using statistical tests.

First, the normality of the distributions was verified. One of the most common continuous probability distribution function is the normal probability density (Figure 2.18), also known as the normal distribution or Gaussian distribution. In statistics, the normal distribution is important for several reasons, including the fact that various continuous phenomena follow, at least approximately, a normal distribution. Furthermore, the Gaussian distribution can be used to approximate numerous discrete probability distributions. To test the normality of the distributions the Shapiro-Wilk test was used [33]. Through this test, the calculation of the p-value was performed, this number allows to determine if there is a significant difference between a certain quantity and the hypothesized value. The p-value is a measure of the credibility of the null hypothesis H_0 ; in fact, if p is small, it means that the observed value in the sample deviates significantly from what is expected under the null hypothesis. The threshold value α , indicates the significance level of the test. In this reserach it was set at 0.05. Once the p-value is calculated, one can proceed as follows:

- if $p > \alpha$ then we accept the null hypothesis H_0 and we reject the alternative one, therefore we suppose that the data are normally distributed;
- if $p < \alpha$ then we reject the null hypothesis H_0 and we accept the alternative one, therefore we suppose that the data are non-normally distributed.

During the analysis the homoscedasticity of the data was checked using the Bartlett test [34], which determines whether multiple samples come from populations with equal variances.

Some statistical tests, such as the T-test, require that variances are equal among groups or samples. Variance is a statistical variable that defines the average of the squares of the differences between individual values of the population and

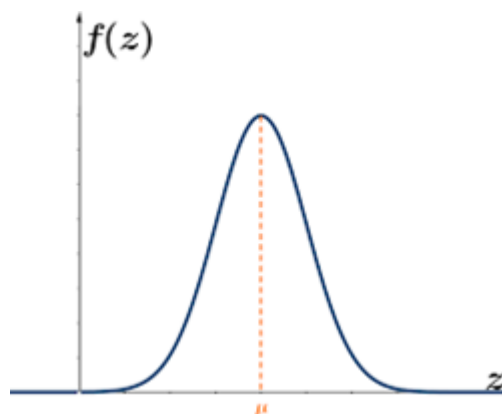


FIGURE 2.18: Normal probability density, reproduced from [32].

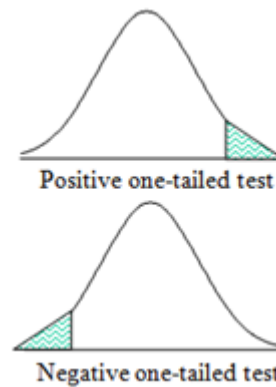


FIGURE 2.19: One-tailed test, adapted from [36].

their arithmetic mean.

After confirming the normality and homoscedasticity of the distributions, the T-test was applied. It is a statistical test used to compare the means of two groups; for the purpose of this research, the mean values of the estimated parameteres, for the different configurations, were compared. The T-test [35] is a parametric test and is used when the samples meet the conditions of normality and equal variance.

The test was done comparing different configurations using the function TEST.T in Microsoft Excel. After having selected the two data distributions for the test, the function required to specify the "tail" and the "type" of test to apply.

A "one-tailed" test refers to a test in which the critical region, so the rejection region, appears only on one end of the distribution. "One-tailed" hypothesis tests are also known as directional tests because the effects are tested in only one direction. When a one-tailed test is performed, the entire significance level percentage goes into the extreme end of one tail of the distribution. It signifies that the estimated test parameter can be greater or lower than the critical value.

A "one-tailed" test (Figure 2.19) can be:

- left-tailed test (negative "one-tailed" test): it is used when the alternative hypothesis states that the true value of the parameter specified in the null hypothesis is less than the null hypothesis claims;
- right-tailed test (positive "one-tailed" test): it is used when the alternative hypothesis states that the true value of the parameter specified in the null hypothesis is greater than the null hypothesis claims.

In a "two-tailed" test (Figure 2.20), the rejection region or critical area is located on both ends of the normal distribution. It determines if the sample falls within a certain range of values. α represents the significance level of the test and is set at 0.05 but since it is a "two-tailed" test the p-value found is compared with 0.025.

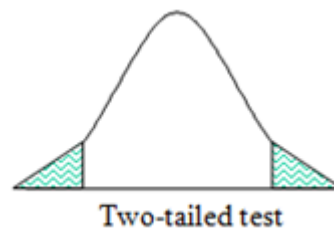


FIGURE 2.20: Two-tailed test, adapted from [36].

When using the Excel function TEST.T the options are:

- paired t-test;
- homoscedastic t-test: it is used when there is equal variance between two samples;
- heteroscedastic t-test: it is used when there is unequal variance between two samples.

For the following analysis the "two-tailed" tests were used with the assumption of homoscedasticity.

Chapter 3

Results and discussions

3.1 Lock/Unlock configuration outcomes

During the treatment the clamps can be used both in lock and unlock configurations according to the surgical technique.

3.1.1 Results

The mean (\pm standard deviation) values evaluated on five samples of IFM and DISP obtained for the different thickness of simulated bone callus (6 mm and 9 mm) are reported in 3.1 and Table 3.2.

6 mm	UNLOCK	LOCK
IFM [mm]	0.258 (± 0.011)	0.228 (± 0.004)
DISP [mm]	0.894 (± 0.005)	0.865 (± 0.008)

TABLE 3.1: 6 mm simulated bone callus results.

9mm	UNLOCK	LOCK
IFM [mm]	0.287 (± 0.013)	0.259 (± 0.001)
DISP [mm]	0.859 (± 0.006)	0.846 (± 0.004)

TABLE 3.2: 9 mm simulated bone callus results.

3.1.2 Statistical results

The distributions of the data (IFM and DISP) obtained from the mechanical tests are normal both for the case of 6 mm simulated bone callus and 9 mm. The values of the p -value_{Shapiro Wilk test} are reported in Table 3.3 and Table 3.4, they are always greater than 0.05 (level of significance of the test) therefore the data do not show a significant departure from normality.

	p-value _{Shapiro Wilk test}
IFM unlock	0.45
DISP unlock	0.29
IFM lock	0.47
DISP lock	0.75

TABLE 3.3: Shapiro Wilk Test's p -value for 6 mm Simulated Bone Callus Data.

	p-value _{Shapiro Wilk test}
IFM unlock	0.08
DISP unlock	0.32
IFM lock	0.24
DISP lock	0.28

TABLE 3.4: Shapiro Wilk Test's p -value for 9 mm Simulated Bone Callus Data.

Then using the T-test it was possible to conclude that values obtained for IFM and DISP comparing Lock and Unlock configurations are statistically different.

3.1.3 Discussions

Considering 6 mm simulated bone callus the collected data shows variations statistically different for:

- IFM decreases of 11.6% from UNLOCK (0.258 mm) to LOCK (0.228 mm) configuration (p -value = 4.09×10^{-7});
- DISP decreases of 3.24% from UNLOCK (0.894 mm) to LOCK (0.865 mm) configuration (p -value = 3.17×10^{-6}).

Considering the 9 mm simulated bone callus data shows:

- IFM decreases of 9.7% from UNLOCK (0.287 mm) to LOCK (0.259 mm) configuration (p -value = 1.12×10^{-5});
- DISP decreases of 1% from UNLOCK (0.859 mm) to LOCK (0.846 mm) configuration (p -value = 5.3×10^{-3}).

We can assume that the applied load is distributed more on the fixator frame rather than on the simulated bone callus in LOCK compared to UNLOCK configuration since both the IFM and DISP show decreased values.

In according to this statement the data shows:

- with 6 mm of simulated bone callus the global stiffness increases of 4% in LOCK configuration;
- with 9 mm of simulated bone callus the global stiffness increase of 1.5% in LOCK configuration.

Considering the lock configuration for the two simulated bone callus, as reported in the Figure 3.1, the 9 mm simulated bone callus setup shows higher IFM but lower DISP compared to the 6 mm simulated bone callus (both p-values < 0.05).

It has to be noticed that the test setup acquires axial displacement exclusively. As described in literature movements in the sagittal plane occur [14] [17] [18] and we can assume that these movements influence the DISP values, but we are not able to quantify them with the current setup.

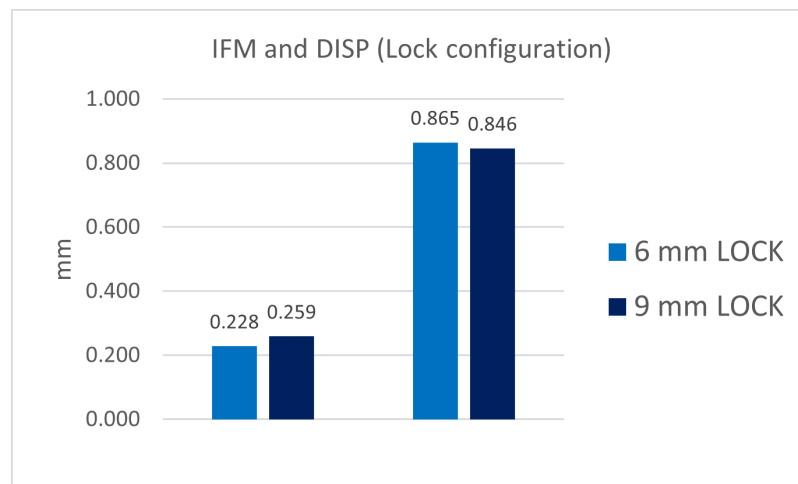


FIGURE 3.1: IFM and DISP obtained from the lock configuration.

3.2 Simulated bone callus outcomes

3.2.1 Results

Executing the test considering the simulated bone callus as is explained above (Paragraph 2.3.2) we can state that (Figure 3.2):

- moving from 6 mm of simulated bone callus to 10.3 mm so an increase of 70% in thickness cause an increase in DISP of 50%;
- moving from 10.3 mm of simulated bone callus to 16.3 mm so an increase of 58% in thickness cause an increase in DISP of 37%;
- moving from 16.3 mm of simulated bone callus to 21.2 mm so an increase of 30% in thickness cause an increase in DISP of 13%.

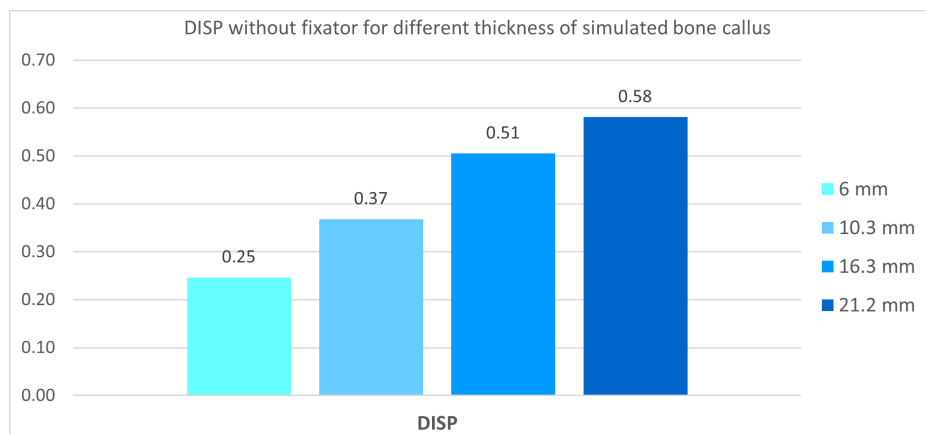


FIGURE 3.2: DISP without the application of the fixator.

3.2.2 Statistical results

The distributions of the data obtained from the mechanical tests are normal for all the thickness of simulated bone callus, this hypothesis was verified applying the Shapiro Wilk Test and having found $p\text{-value}_{\text{Shapiro Wilk test}}$ always greater than 0.05 (Table 3.5).

DISP	$p\text{-value}_{\text{Shapiro Wilk test}}$
6 mm	0.94
10.3 mm	0.33
16.3 mm	0.62
21.2 mm	0.08

TABLE 3.5: Shapiro Wilk Test's p-value for Different Thicknesses of Simulated Bone Callus.

Then using the T-test it was possible to conclude that values obtained for DISP are statistically different in the case of simulated bone callus with thickness of 6, 10.3, 16.3 and 21.2 mm as visible from the p -value_{Shapiro Wilk test} obtained (Table 3.6) from each comparison always lower than 0.05.

Comparison	p -value _{T-test}
DISP (6 mm VS 10.3 mm)	2.09×10^{-10}
DISP (6 mm VS 16.3 mm)	1.29×10^{-12}
DISP (6 mm VS 21.2 mm)	3.87×10^{-14}
DISP (10.3 mm VS 16.3 mm)	1.77×10^{-10}
DISP (10.3 mm VS 21.2 mm)	1.01×10^{-12}
DISP (16.3 mm VS 21.2 mm)	1.10×10^{-8}

TABLE 3.6: T-test p -values for Each Comparison

3.2.3 Discussions

Increasing the thickness of the simulated bone callus DISP increases as well. We can assume that the structure with 21.2 mm simulated bone callus is less stiff than the 6 mm model. To bring out the fact that increasing the thickness of the simulated bone callus DISP increases as well are done tests placing the Sawbones of 6, 10.3, 16.3 and 21.1 mm in the gap between the two tibial segments after the osteotomy. If increasing the thickness DISP increase the axial stiffness (E) decrease, graphs are reported in the figure below (Figure 3.3).

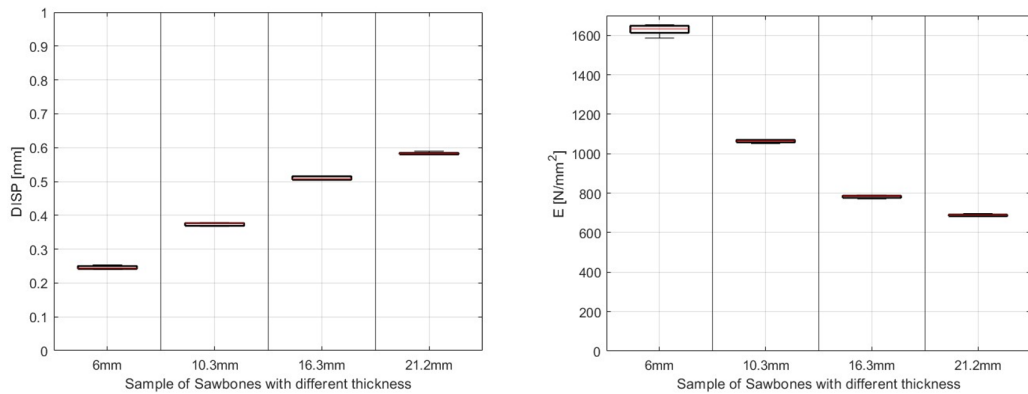


FIGURE 3.3: From left to right: boxplot representing DISP and E obtained in different tests with increasing thickness of Sawbones (6 mm ÷ 21.2 mm).

It is possible to find a correlation between the mean values of each test for DISP and E as shown in the Figure 3.4.

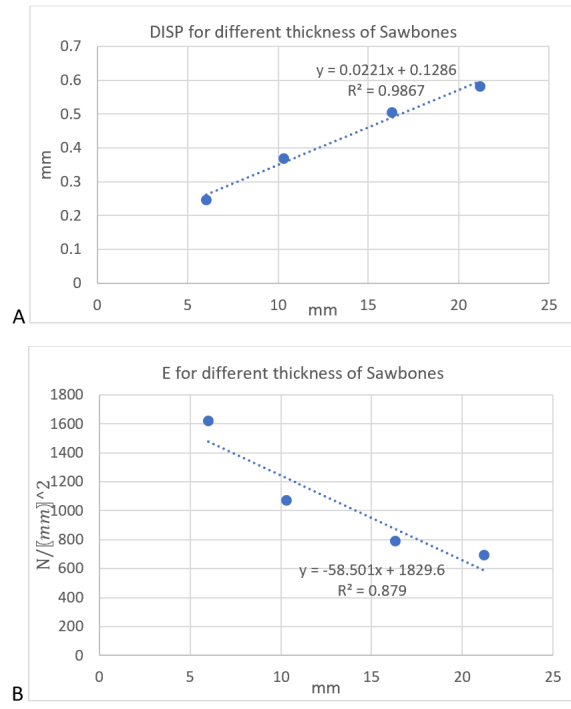


FIGURE 3.4: A: regression line obtained starting from the mean values of DISP for each test, B: regression line obtained starting from the mean values of E for each test. In both cases tests are done with increasing thickness of Sawbones (6 mm ÷ 21.2 mm).

R-squared is an index that has a value between 0 and 1. Values close to 1, like the one found in the previous graphs, indicate that much of the variation of the dependent variables (DISP and E values) can be explained by the linear regression model used. In other words, the linear regression model is able to explain and predict much the variation in the data of the dependent variables. The fact that was possible to find a linear regression model help to understand what happens when the thickness of the simulated bone callus is increased. This allow to approximate the behavior of the Sawbones with the formula:

$$\delta = \frac{P \cdot L}{E \cdot A}$$

where P is the axial load applied to the structure; L is the different thickness of the regenerated bone callus, A is the area of the section of where the load is applied and E is the Elastic modulus of the material underwent the test. It has to be noticed that this formula derived from any situation in which a homogeneous, isotropic metal rod of length L and constant cross-sectional area A is subjected to a concentrated axial load P. In the present study we use it to explain the linear behaviour of the simulated bone callus subjected to compressive test.

3.3 Rekreia Tandem configuration outcomes

Considering the test performed in Tandem configuration we obtain different results depending on:

- Frame Configuration (AnteroPosterior or MedioLateral application);
- Stage of healing process (6 or 9 mm simulated bone callus) (Figure 3.5);
- Bone screw configuration (number/position of pins in the mobile clamps).

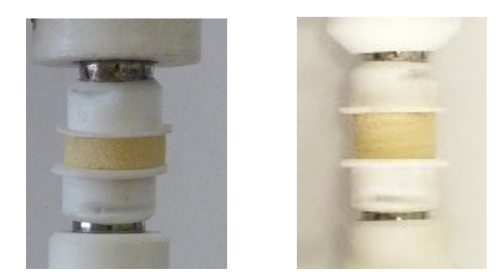


FIGURE 3.5: From left to right: Sawbones to simulate the bone callus with thickness of 6 mm and 9 mm.

3.3.1 Results for the MedioLateral application of the fixator

In this phase of the test the fixator is positioned with 45° of inclination respect to the sagittal plane (Figure 3.6). This setup is tested in order to try to better counteract the moments developed by muscles and tendons (Figure 1.12, Paragraph 1.2.3) [14].

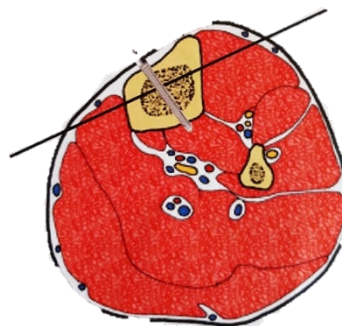


FIGURE 3.6: Tibial fixation with a mediolateral wire.

Considering that positioning of the device with two pins in the central clamp (Td_central_2screws) or in the distal one (Td_distal_2screws), analysing the results they were not so different in terms of DISP (0.628 mm, 0.625 mm) (-0.5%, p-value = 5.5×10^{-3}) in case of 6 mm of regenerated bone.

Moving from Td_central_2screws to Td_distal_2screws was obtained an increase in IFM (0.101 mm, 0.103 mm) (+2%, p-value = 2.53×10^{-4}) (Figure 3.7).

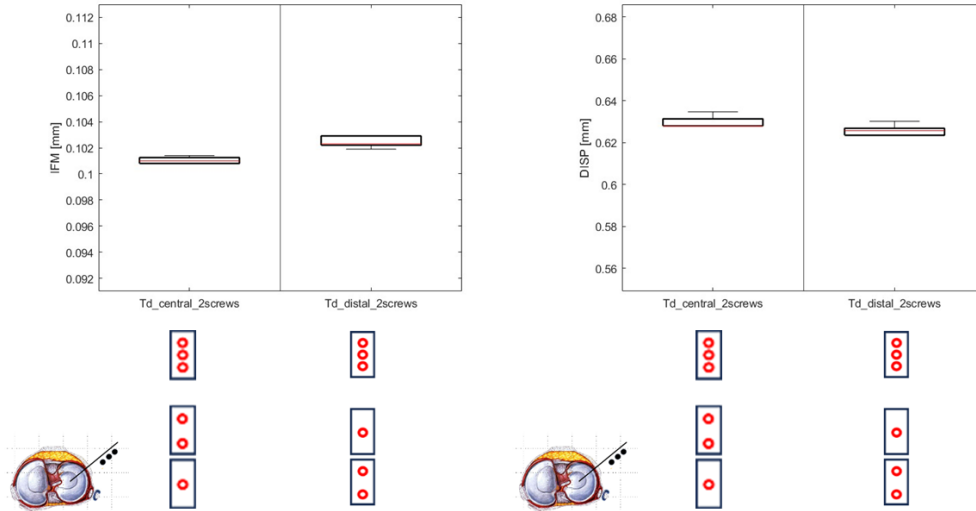


FIGURE 3.7: From the left to the right: IFM and DISP in the two configurations reported above with 6 mm of simulated bone callus.

With 6 mm of simulated bone callus if we compare Td_central_full and Td_distal_full (three pins in the central or distal clamps) analysing the IFM we had no difference between the two (p-value = 0.91) and DISP was quite similar (0.62 mm, 0.60 mm) (-3%, p-value = 2.34×10^{-6}) (Figure 3.8).

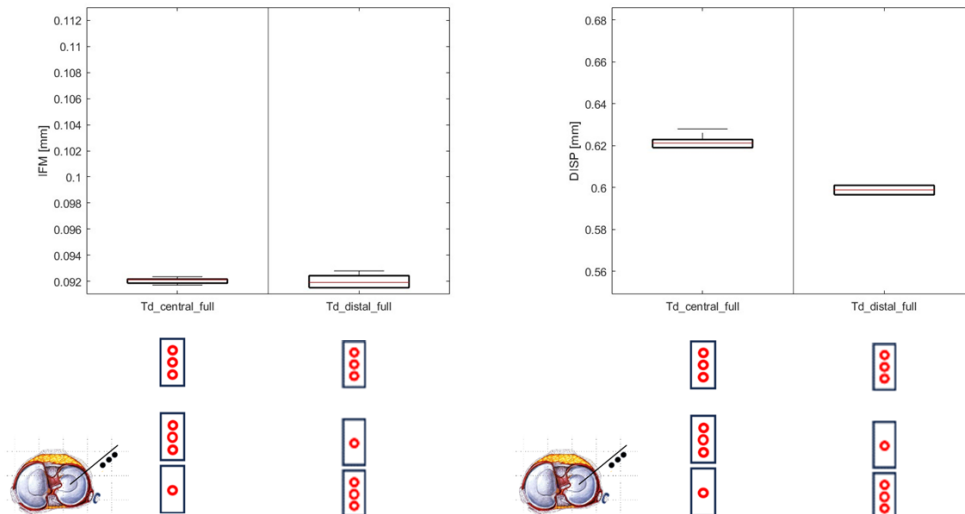


FIGURE 3.8: From the left to the right: IFM and DISP in the two configurations reported above with 6 mm of simulated bone callus.

If we considered simulated bone callus of thickness of 9 mm moving from Td_central_2screws to Td_distal_2screws was obtained a decrease in terms of IFM (0.145 mm, 0.125 mm) (-13%, p-value = 4.82×10^{-15}) and of DISP (0.708 mm, 0.675 mm) (-4.6%, p-value = 2.70×10^{-6}) (Figure 3.9).

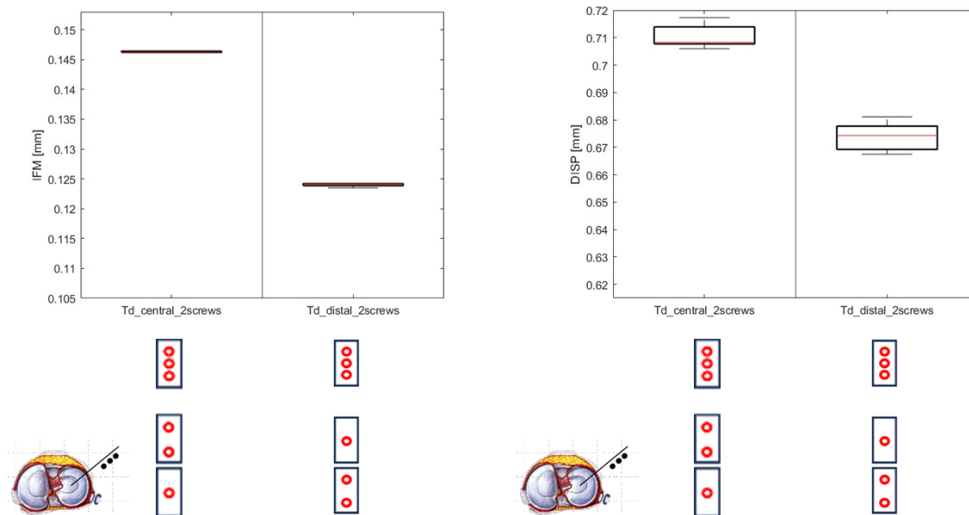


FIGURE 3.9: From the left to the right: IFM and DISP in the two configurations reported above with 9 mm of simulated bone callus.

With 9 mm of bone callus moving from Td_central_full to Td_distal_full was obtained a decrease in terms of IFM (0.110 mm, 0.107 mm) (-3%, p-value = 0.02) and of DISP (0.643 mm, 0.633 mm) (-1.6%, p-value = 0.001) (Figure 3.10).

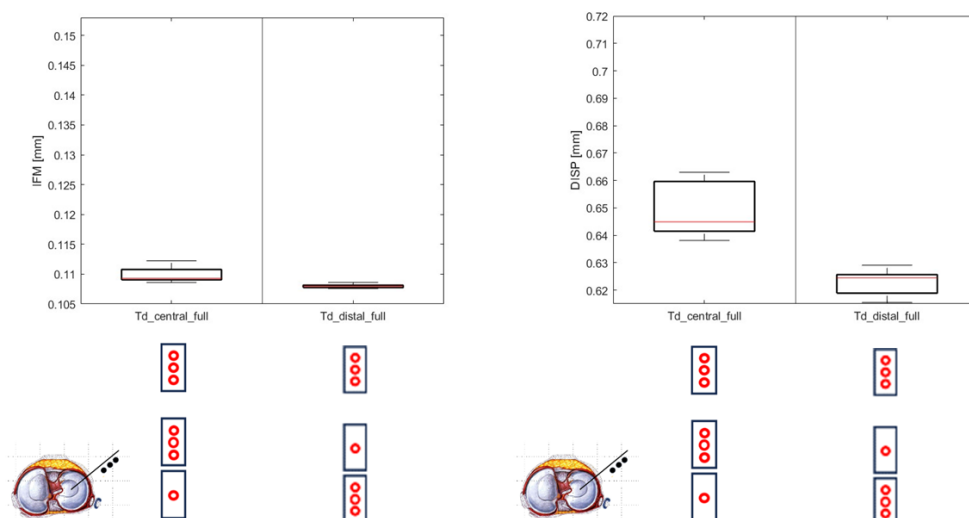


FIGURE 3.10: From the left to the right: IFM and DISP in the two configurations reported above with 9 mm of simulated bone callus.

Further results were shown from the comparison between Td_distal_2screws and Td_distal_full or Td_central_2screws and Td_central_full, both in terms of IFM and DISP, for 6 mm and 9 mm of simulated bone callus.

Starting from 6 mm of thickness moving from Td_distal_2screws to Td_distal_full was obtained a decrease in IFM (0.102 mm, 0.092 mm) (-10%, p-value = 7.61×10^{-10}) and DISP (0.625 mm, 0.60 mm) (-4%, p-value = 1.49×10^{-7}) (Figure 3.11).

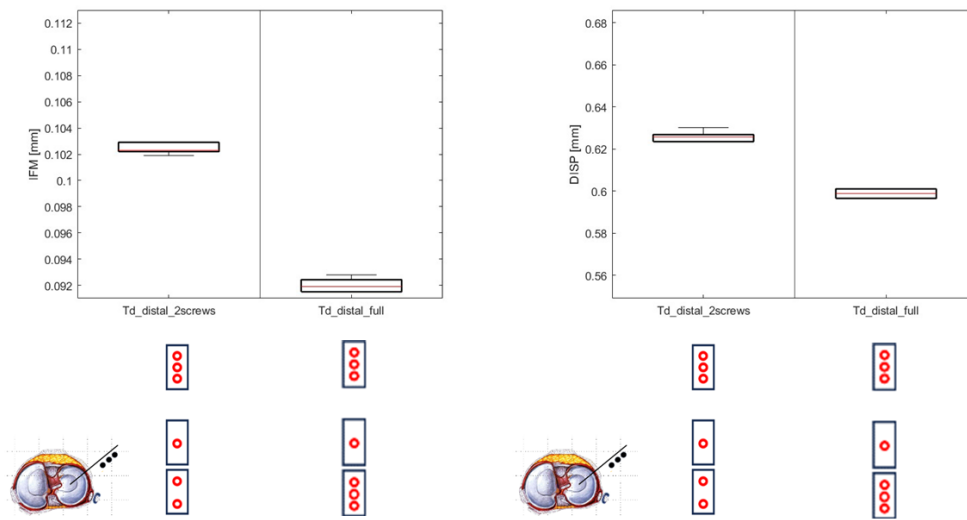


FIGURE 3.11: From the left to the right: IFM and DISP in the two configurations reported above with 6 mm of simulated bone callus.

Always with simulated bone callus of 6 mm moving from Td_central_2screws to Td_central_full was obtained a decrease in IFM (0.105 mm, 0.092 mm) (-12%, p-value = 1.03×10^{-11}) and DISP (0.634 mm, 0.628 mm) (-1%, p-value = 4.8×10^{-3}) (Figure 3.12).

Considering 9 mm of thickness for the simulated bone callus moving from Td_distal_2screws to Td_distal_full was obtained a decrease in IFM (0.124 mm, 0.107 mm) (-14%, p-value = 1.38×10^{-12}) and DISP (0.675 mm, 0.635 mm) (-6%, p-value = 2.5×10^{-4}) (Figure 3.13).

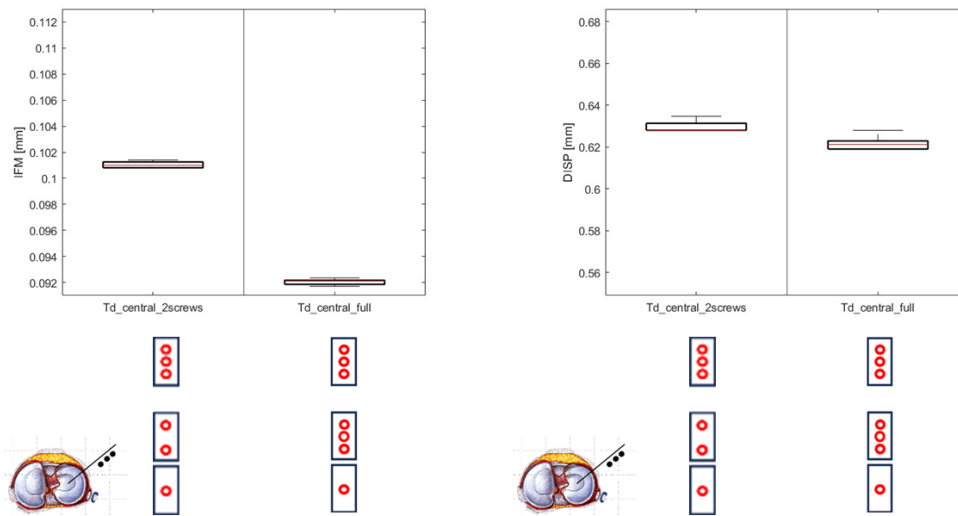


FIGURE 3.12: From the left to the right: IFM and DISP in the two configurations reported above with 6 mm of simulated bone callus.

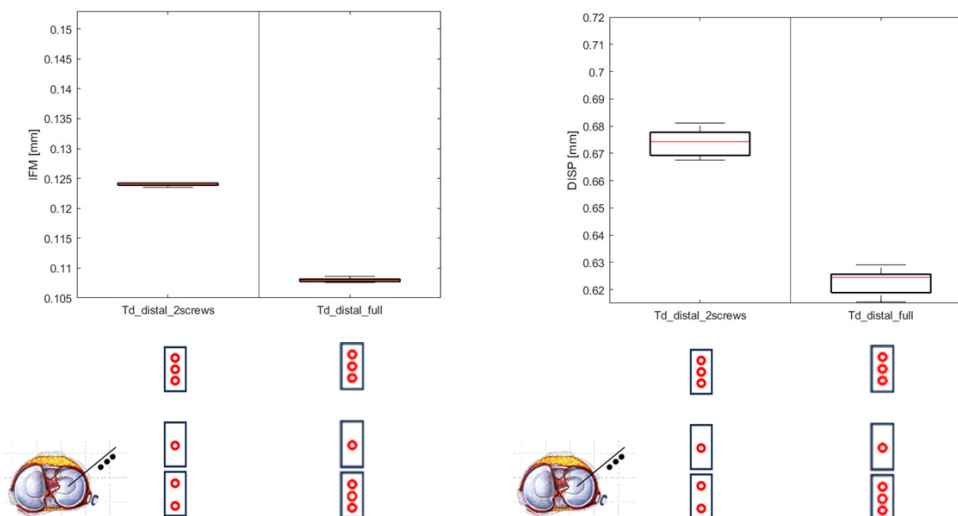


FIGURE 3.13: From the left to the right: IFM and DISP in the two configurations reported above with 9 mm of simulated bone callus.

Having fixed 9 mm of thickness for the simulated bone callus moving from Td_central_2screws to Td_central_full was obtained a decrease in IFM (0.146 mm, 0.107 mm) (-27%, $p\text{-value} = 1.02 \times 10^{-11}$) and DISP (0.708 mm, 0.645 mm) (-8%, $p\text{-value} = 2.56 \times 10^{-6}$) (Figure 3.14).

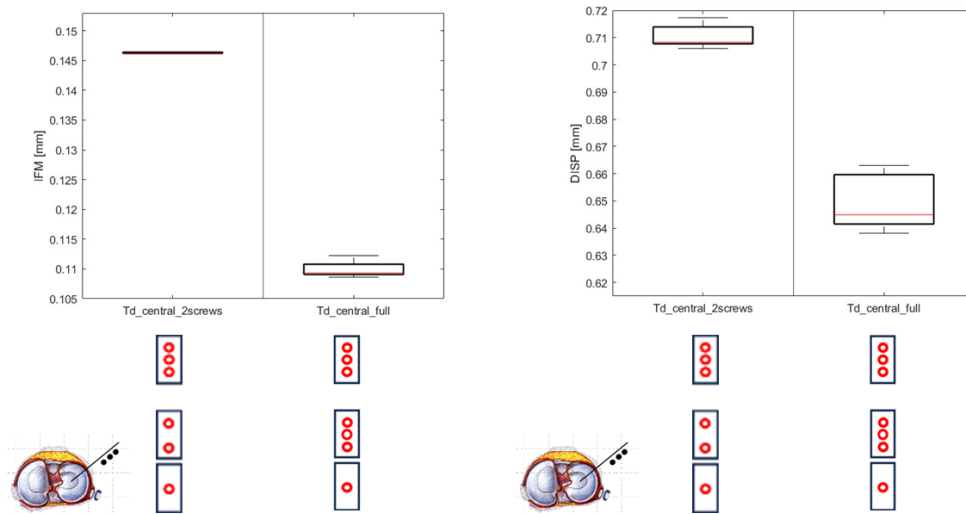


FIGURE 3.14: From the left to the right: IFM and DISP in the two configurations reported above with 9 mm of simulated bone callus.

3.3.2 Results from the AnteroPosterior application of the fixator

With 6 mm of regenerated bone, if we consider two screws in the distal clamp (Td_distal_2screws) instead of the central clamp (Td_central_2screws) we can conclude that the first configuration was stiffer than the second one. In particular from Td_distal_2screws to Td_central_2screws we had an increase in IFM (0.096 mm, 0.102 mm) (+6%, p-value = 8.34×10^{-6}) and DISP (0.565 mm, 0.609 mm) (+7.8%, p-value = 8.17×10^{-8}) (Figure 3.15).

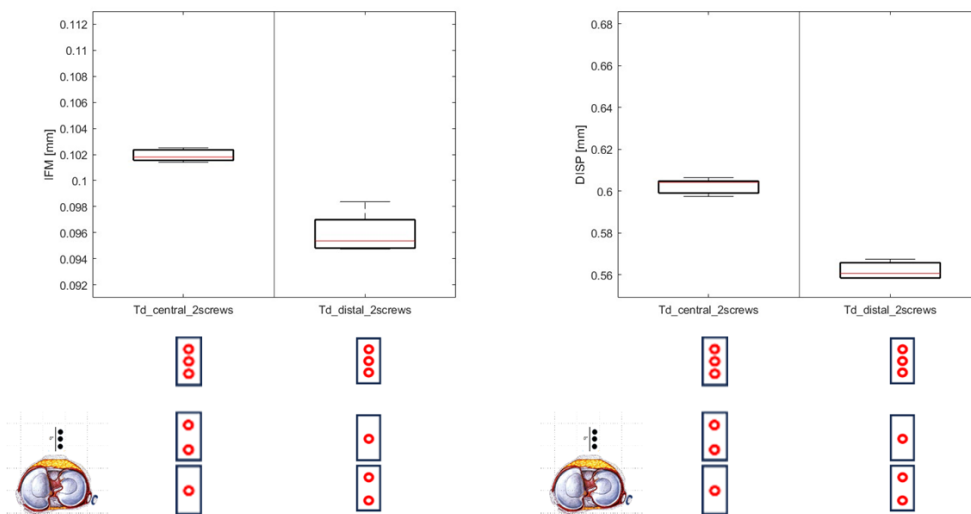


FIGURE 3.15: From the left to the right: IFM and DISP in the two configurations reported above with 6 mm of simulated bone callus.

Adding a bone screw in the central or in the distal clamp, we obtain a similar trend since data show that distal configuration is stiffer than the central configuration.

Moving from Td_distal_full to Td_central_full we have an increase in IFM (0.107 mm, 0.111 mm) (+4%, p-value = 2.56×10^{-6}) and DISP (0.655 mm, 0.675 mm) (+3%, p-value = 1.86×10^{-6}) as shown in the graph below (Figure 3.16).

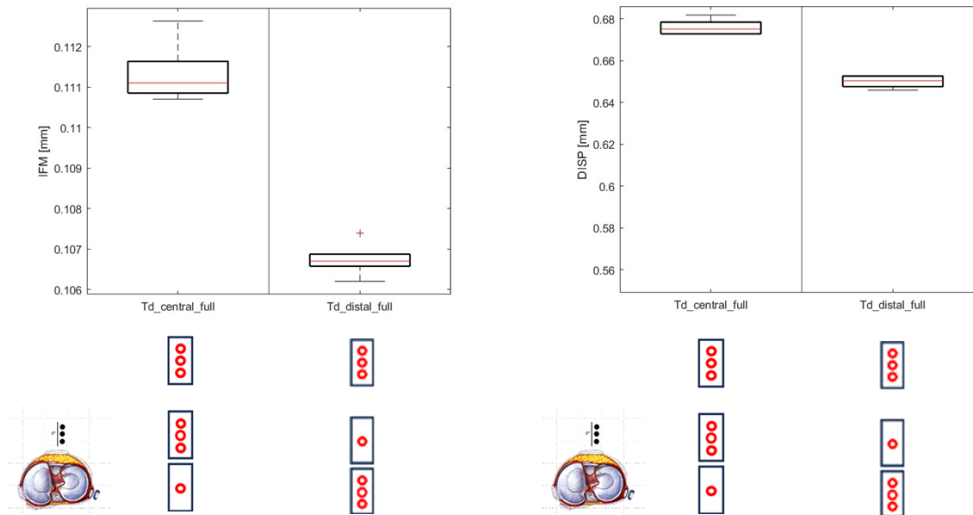


FIGURE 3.16: From the left to the right: IFM and DISP in the two configurations reported above with 6 mm of simulated bone callus.

Simulating few days later in the treatment, results were confirmed also in the case of 9 mm simulated bone callus (Figure 3.17).

Moving from Td_distal_2screws to Td_central_2screws was obtained an increase in IFM (0.116 mm, 0.150 mm) (+29%, p-value = 4.37×10^{-12}) and DISP (0.64 mm, 0.71 mm) (+10%, p-value = 1.81×10^{-8}).

Instead moving from Td_distal_full to Td_central_full we had an increase in IFM (0.123 mm, 0.129 mm) (+5%, p-value = 5.01×10^{-7}) and DISP (0.664 mm, 0.695 mm) (+4.5%, p-value = 7.2×10^{-5}) as showed by the graph below: Figure 3.18.

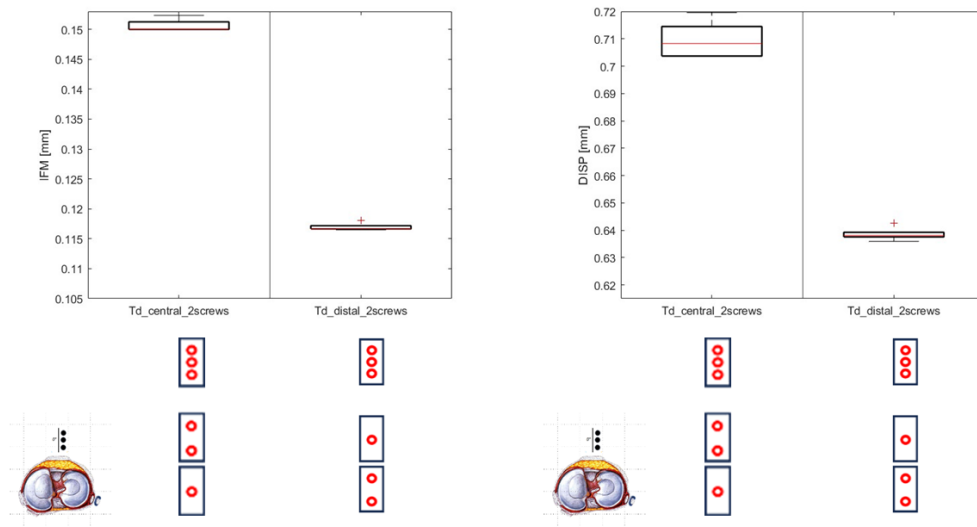


FIGURE 3.17: From the left to the right: IFM and DISP in the two configurations reported above with 9 mm of simulated bone callus.

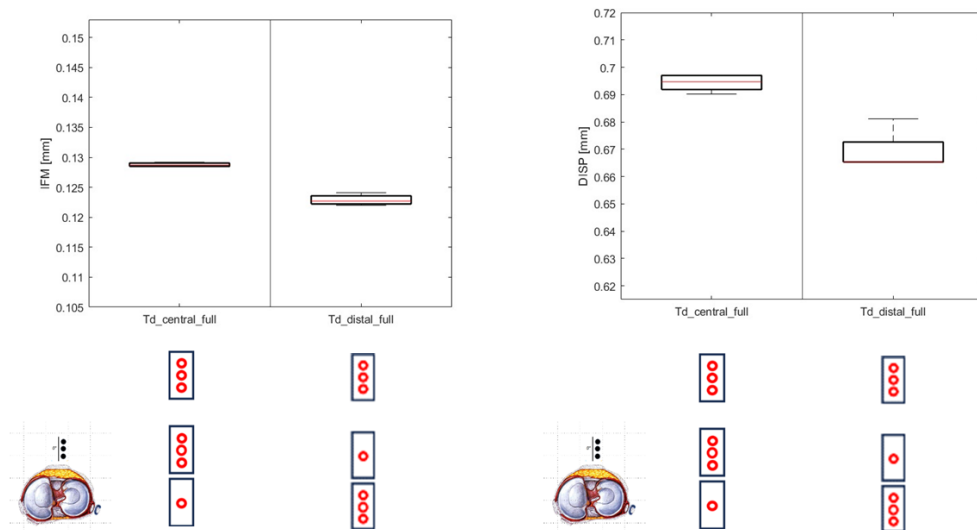


FIGURE 3.18: From the left to the right: IFM and DISP in the two configurations reported above with 9 mm of simulated bone callus.

Comparing the same configuration “Td_distal” with 6 mm of simulated bone callus, but varying the number of the bone screws, two or three pins in the distal clamp (Td_distal_2screws or Td_distal_full) (Figure 3.19) was shown that the first configuration was stiffer, reaching lower values both for IMF and DISP. Moving from Td_distal_2screws to Td_distal_full was obtained an increase in IFM (0.095 mm, 0.106 mm) (+11%, p-value = 5.8×10^{-8}) and DISP (0.565 mm, 0.65 mm) (+15%, p-value = 5.49×10^{-11}).

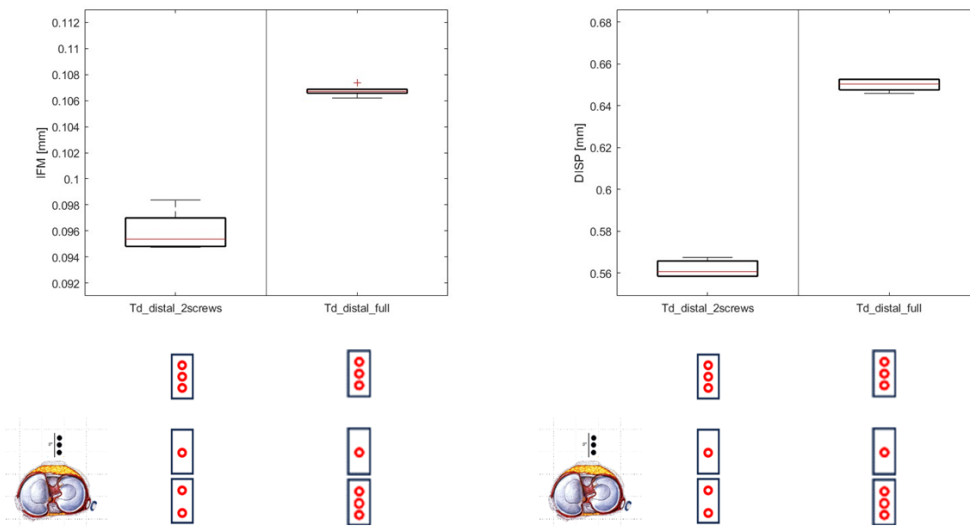


FIGURE 3.19: From the left to the right: IFM and DISP in the two configurations reported above with 6 mm of simulated bone callus.

Similarly, always with 6 mm of simulated bone callus, between Td_central_2screws and Td_central_full is added one pin in the central clamp and considering the graph of IFM and DISP (Figure 3.20), moving from Td_central_2screws to Td_central_full was obtained an increase in IFM (0.102 mm, 0.1119 mm) (+9.8%, p-value = 1.15×10^{-11}) and DISP (0.61 mm, 0.679 mm) (+11.5%, p-value = 1.23×10^{-9}).

This behaviour, in case the material between the two bone segments had a thickness of 9 mm, so simulating the test few days later in the treatment, was confirmed only in the comparison between Td_distal_2screws and Td_distal_full. In detail moving from Td_distal_2screws to Td_distal_full was obtained an increase in IFM (0.117 mm, 0.123 mm) (+5%, p-value = 1.43×10^{-6}) and DISP (0.639 mm, 0.667 mm) (+4.7%, p-value = 1.29×10^{-5}) (Figure 3.21).

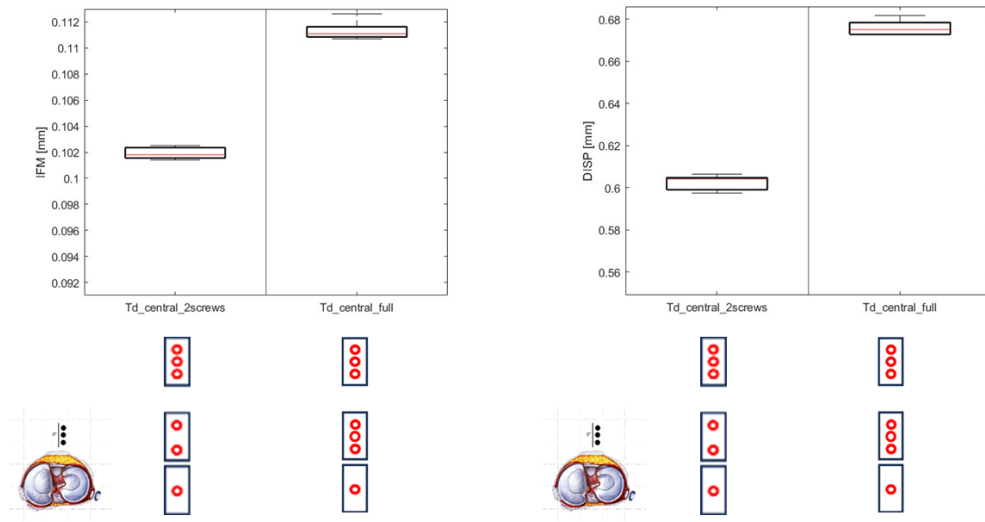


FIGURE 3.20: From the left to the right: IFM and DISP in the two configurations reported above with 6 mm of simulated bone callus.

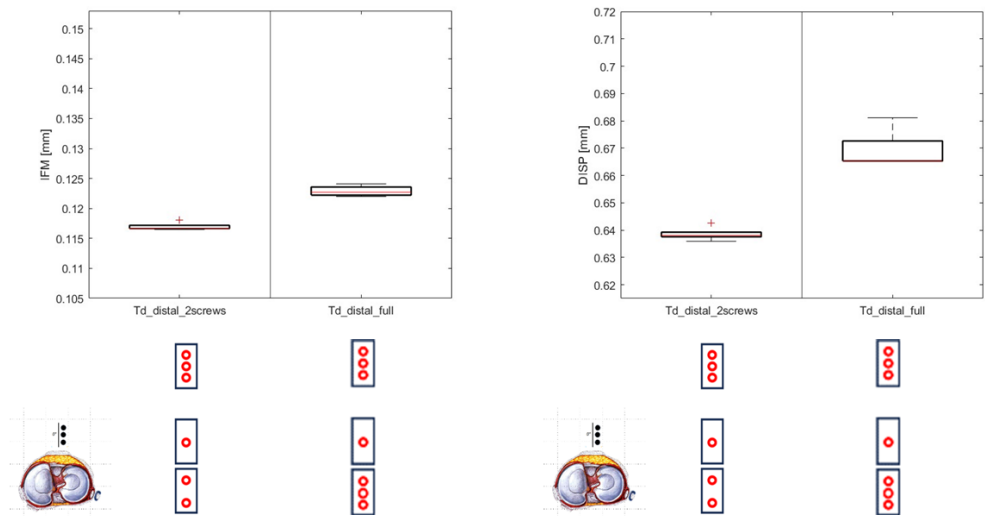


FIGURE 3.21: From the left to the right: IFM and DISP in the two configurations reported above with 9 mm of simulated bone callus.

While, always moving with 9 mm of simulated bone callus, from Td_central_2screws to Td_central_full was obtained a decrease in IFM (0.151 mm, 0.128 mm) (-15%, $p\text{-value} = 5.78 \times 10^{-11}$) and DISP (0.709 mm, 0.689 mm) (-3%, $p\text{-value} = 1.6 \times 10^{-3}$) (Figure 3.22).

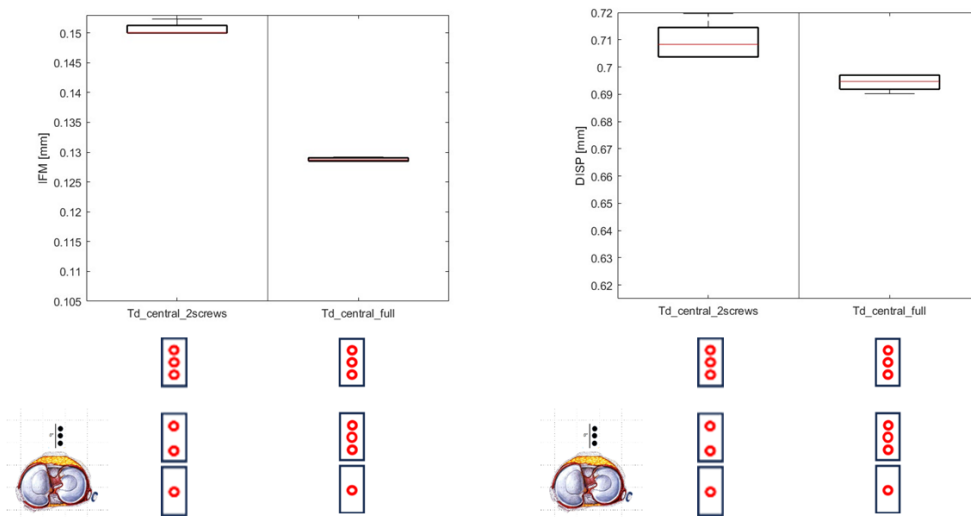


FIGURE 3.22: From the left to the right: IFM and DISP in the two configurations reported above with 9 mm of simulated bone callus.

3.3.3 Statistical results

The distributions of the data obtained from the mechanical tests are normal both for the case of 6 mm and 9 mm, this hypothesis was verified applying the Shapiro Wilk Test and having p-values greater than 0.05. Then using the T-test it was possible to find configurations that are similar so for which the results in terms of IFM and DISP are not statistically different so when the p-value find is greater than the significance level α ; in all other cases the p-value obtained is less than α . Among the configurations where thickness of the simulated bone callus is 6 mm no statistical differences in IFM are highlighted between:

- Td_distal_2screws (ML) and Td_central_2screws (AP) (p-value = 0.09);
- Td_distal_full (ML) and Td_central_full (ML) (p-value = 0.91).

In terms of DISP no statistical differences are highlighted between:

- Td_distal_full (ML) and Td_central_2screws (AP) (p-value = 0.11);
- Td_distal_2screws (ML) and Td_central_2screws (ML) (p-value = 0.05);
- Td_distal_2screws (AP) and Td_distal_full (AP) (p-value = 0.63);
- Td_distal_2screws (ML) and Td_central_full (ML) (p-value = 0.08).

Regarding configurations where thickness of the simulated bone callus is 9 mm statistical differences in IFM are present in each comparison, while in terms of DISP no statistical differences are highlighted between:

- Td_central_2screws (AP) and Td_central_2screws (ML) (p-value = 0.81);
- Td_distal_2screws (AP) and Td_central_full (ML) (p-value = 0.06);
- Td_distal_2screws (ML) and Td_distal_full (AP) (p-value = 0.28).

Comparing the results when the thickness of simulated bone callus is 6 mm against the case in which that layer is 9 mm in terms of IFM no statistical difference have arisen between:

- Td_central_full (AP, 6mm) and Td_central_full (ML, 9mm) (p-value = 0.09).

In terms of DISP no statistical differences have arisen between:

- Td_distal_2screws (ML, 6mm) and Td_distal_full (ML, 9mm) (p-value = 0.28);
- Td_central_full (AP, 6mm) and Td_distal_2screws (ML, 9mm) (p-value = 0.49);
- Td_central_full (AP, 6mm) and Td_distal_full (AP, 9mm) (p-value = 0.10);

- Td_central_full (ML, 6mm) and Td_distal_full (ML, 9mm) (p-value = 0.72);
- Td_distal_full (AP, 6mm) and Td_central_full (ML, 9mm) (p-value = 0.92).

When no statistically significant differences emerge in the comparisons between configurations, it means that for these the number of bone screws and their positioning relative to the tibial axis balance the moments generated during the treatment in a similar way. With the same outcome, it is preferable to use the configuration that requires the fewest number of bone screws.

3.3.4 Discussions

Considering the ML application of the device, the distal configurations showed stiffer behaviour compared to the central configurations: we assume that the insertion of a large number of screws in the central clamp rather than the distal one may cause movements in the transverse plane, therefore movements that are not detectable in our setup.

In general the insertion of three bone screws, rather than two, in the central or distal clamp, comparing the results between Td_distal_2 screws and Td_distal_full or Td_central_2screws and Td_central_full, increases the stiffness in terms of IFM or DISP in case of 6 mm and 9 mm of thickness of regenerated bone in the gap between the two bone segments.

It is possible to conclude that the distal configuration is stiffer than the central one in terms of both IFM and DISP (difference not always statistically significant for the 6 mm simulated bone callus) (Figure 3.23,A-B) and this can be explained by stating that in the distal configuration the lever arm, from the last of the distal bone screws to the ankle joint, is smaller.

Comparing 2screws versus full configurations, the first are less stiff (difference not always statistically significant for the 6 mm simulated bone callus) (Figure 3.23, A-B), although the values obtained are also in agreement with the reference values found in the literature [26] [27].

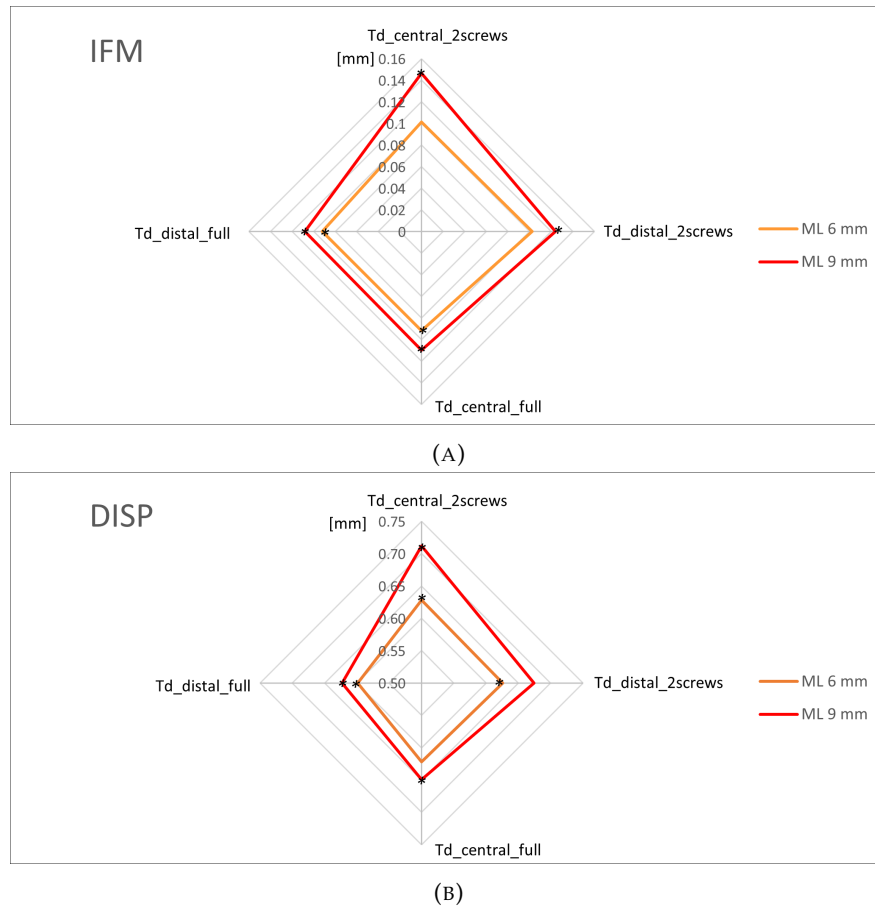


FIGURE 3.23: Radar plot for the ML application of the fixator. Are graphed IFM values (A) and DISP values (B) for all the configurations tested in case of simulated bone callus of 6 and 9 mm.

* denotes significant difference when compared with the anatomical group.

Considering the AP application of the device, comparing Td_central_2screws with Td_distal_2screws (for 6 and 9 mm) is possible to notice that Td_distal_2screws, that appears as the more stiff in the comparison, we can assume that the load is more distributed on the fixator than on the callus itself.

This last consideration is feasible also when in the central or in the distal clamp are present three pins: Td_central_full and Td_distal_full.

To conclude having more pins in the distal clamp instead of in the central one give strength to the implanted system in that precise configurations.

This is true if the regenerated bone placed in the gap between the two bone segments has a thickness of 6 mm or 9 mm; to confirm this last sentence the tests have been done with both the thickness so simulating a situation of bone's growth from 6 to 9 mm, the data have been analysed and the results are shown in the paragraph above (Figures 3.15, 3.16, 3.17, 3.18).

Furthermore from Figure 3.23 merged that when are placed in the gap 9 mm of simulated bone callus the system is more yielding respect to the case in which that layer has a thickness of 6 mm.

It should be noticed that in the case of distal configurations, the lever arm from the last of the distal bone screws to the ankle joint is smaller.

Despite the increased clamp distance L (Figure 3.24), that represents the exposed bending part of the frame, there is an increase in stiffness (and lower IFM) when moving from central to distal configurations. This behaviour is hypothesized to be attributable to the Tandem configuration: the clamp in the center of the frame prevents the frame from bending while maintaining IFM values in line with those suggested by the scientific literature [[26],[27]]. In accordance with what is exposed above we have found Figure 3.24, which referred to a simplified scheme of a modular fixator.

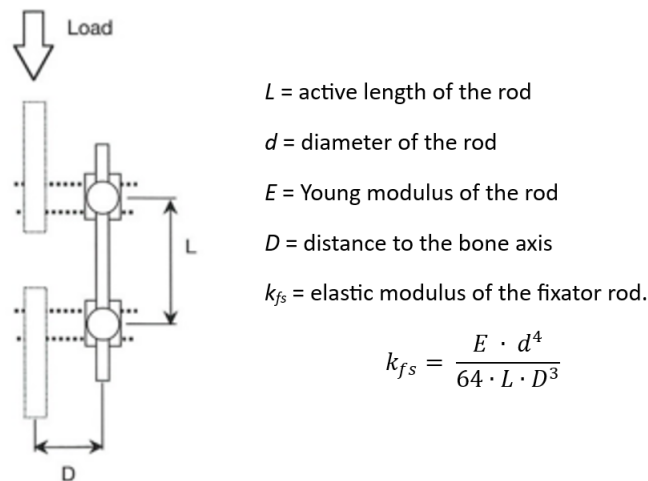


FIGURE 3.24: Scheme of the fixator applied to the bone.

Having the AP application of the device, comparing the central and distal configurations, the trend seen for the ML application of the device is confirmed, thus that the distal ones are stiffer (difference not always statistically significant in DISP with 9 mm simulated bone callus) (Figure 3.25, B).

Regarding the comparison between 2screws and full configurations when in the fracture gap are present 6 mm of simulated bone callus the behaviour was not in good accordance with ML application results (Figure 3.25, A-B) and also with 9 mm of simulated bone callus the behaviour was not in accordance with ML configuration results.

This fact can be explained knowing the complexity of the moment that were generated with this setup; therefore for future investigations it would be appropriate to use a setup that allows for the evaluation of not only axial movements.

In conclusion the 9 mm test sessions exhibit greater data dispersion due to both a greater exposed length of the frame bars and the thickness of the Sawbones placed in the fracture gap (Paragraph 3.1.1). In addition when three pins are involved both in the central or in distal clamps moving from the AP application to the ML application is more rigid having lower IFM and DISP.

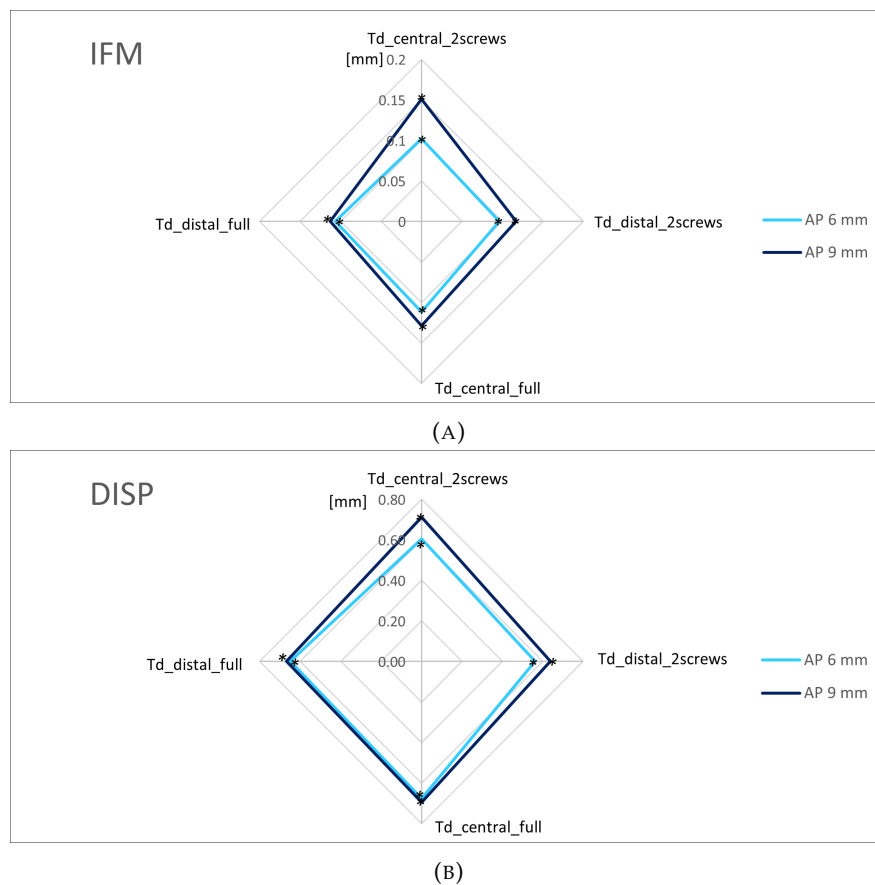


FIGURE 3.25: Radar plot for the AP application of the fixator. Are graphed IFM values (A) and DISP values (B) for all the configurations tested in case of simulated bone callus of 6 and 9 mm.

* denotes significant difference when compared with the anatomical group.

Chapter 4

Conclusions

The current document has the objective to investigate different configurations of the Rekrea fixator used during tibial lengthening treatments. Consequent phases were simulated using different thicknesses for the bone callus placed in the gap of the fracture.

A bibliographic research was done to understand the state of art in the use of the external fixator systems for bone lengthening procedures. It emerged that the loads on the bone callus are critical.

The data analysis of the first test scenario demonstrated how, switching from the Lock to the Unlock configuration, the obtained results were different. In particular, the Lock configuration was stiffer than the Unlock setup, showing smaller IFM and DISP. After, the effects of varying the thickness of the bone callus were analysed. It appeared that, as the thickness of the bone callus increased, the flexibility of the assembly increased too. This meant an increase of the full-scale of the computed values increasing the thickness of the simulated bone callus.

The other configurations (Tandem applications) were tested for 6 mm and 9 mm of simulated bone callus to investigate the onset of the distraction phase, where the forces exerted by the soft tissues were contained, and this was in line with the setup that did not have the contribution of soft tissues.

The first Tandem applications tested had the bone screws inserted parallel to the mediolateral axis of the tibia (ML application), therefore, results from the four configurations of each thickness of bone callus (6 and 9) were obtained. Then, the same four configurations were tested when the screws were inserted parallel to the anteroposterior axis of the tibia (AP application).

Regarding the ML application, it was possible to conclude that, having the possibility to add one pin in the central or distal clamp and comparing the results between Td_central_2screws with Td_central_full and Td_distal_2screws with Td_distal_full, the stiffest situation appeared when the pins were added ("full" configurations) both in terms of IFM or DISP for the different thickness of the bone callus.

This conclusion was not confirmed considering the AP application: the values obtained for IFM and DISP were greater in respect to ML case (this difference was confirmed by statistical analysis).

It was hypothesized that if the system in the central clamp was more flexible, it could develop shear forces that induced non axial movements of the stumps. These were not detectable from the setups used, therefore the values measured with ML applications were smaller.

This last application (AP) could be investigated in other research, without limiting the analysis to the axial movement because soft tissues induced moments on the bone that caused additional deformations, critical during the treatment of elongations.

In the future, tests could also be conducted using materials characterized by behaviour similar to that of the bone tissue. These analyses could lead to results that better approximate a physiological condition. Further analysis could also be done changing the angles of inclination in respect to the tibial axis to find a configuration that limits, as much as possible, the movements caused by shear forces.

Also the difference between the results of all the Tandem configurations obtained with 6 mm and 9 mm of simulated bone callus could benefit from further studies with more complex scenarios.

The outcome of this study was a good starting point to improve the positioning of the Rekrea external fixation device applied on the needs of the patient treated.

List of Figures

1.1	Shape of the osteotomy, reproduced by [3].	10
1.2	Types of osteotomy, reproduced by [3].	10
1.3	Structure of a long bone, reproduced from [4].	11
1.4	Wolff' Law.	12
1.5	Callus formation and bone remodelling, adapted from [7].	13
1.6	The Ilizarov ring fixator, 1951, reproduced from [8].	14
1.7	From left to right: external fixator with circular and unilateral frame, adapted from [9] and [10].	15
1.8	Distraction phase, reproduced from [10].	16
1.9	Mechanical scheme of the system composed by the treated bone and the fixator, adapted from [11].	17
1.10	Transformation of the bone callus during dynamization phase, adapted from [11].	18
1.11	Resultant hip contact force and knee contact force, both in BW, reproduced from [14].	19
1.12	Internal forces in BW (left) and internal moments in BWmm (right) over the gait cycle at the three locations along the tibial axis, reproduced from [14].	20
1.13	Distraction force in time in a tibial lengthening treatment, reproduced from [14].	20
1.14	Force readings after a lengthening of 0.25 mm, reproduced from [14].	20
1.15	Viscoelastic behaviour of soft tissue, adapted from [16].	21
1.16	Distraction force in case of congenitally short limbs (red line) and traumatic shortening (blu line), adapted from [14].	22
1.17	Mechanical (A) and anatomical (B) axis of the entire leg, adapted from [20].	23
1.18	Screw insertion in the proximal part of the tibia, reproduced from [21].	25
1.19	Screw insertion in the distal part of the tibia, reproduced from [21].	25

1.20	Screw insertion in the middle zone of the tibia, reproduced from [21].	25
1.21	Screw insertion in the distal zone of the tibia, reproduced from [21].	26
1.22	Axial stiffness (AS) and interfragmentary movements (IFM) relation.	28
2.1	MTS 632.79 Immersible Extensometer.	31
2.2	Testing machine.	31
2.3	Load in time acting on the structure.	32
2.4	Monolateral Rekrea fixator body, reproduced from [10].	33
2.5	Rekrea Small fixator body, reproduced from [10].	34
2.6	Mobile clamps for Rekrea fixator body and Rekrea Small fixator body, reproduced from [10].	35
2.7	“ON” and “LOCK-UNLOCK” screws of the clamp, reproduced from [10].	35
2.8	Steel double-diameter thread bone screw, reproduced from [10].	36
2.9	Complete system mounted on the testing machine.	37
2.10	System without Rekrea anchored mounted on the testing machine.	38
2.11	Focus on the system without Rekrea.	38
2.12	Configuration Td_central_2screws	39
2.13	Configuration Td_distal_2screws.	39
2.14	Configuration Td_central_full.	40
2.15	Configuration Td_distal_full.	40
2.16	Directions of the insertion of the screws in the bone, adapted from [21].	41
2.17	Anteroposterior and mediolateral positioning of the fixator. . .	41
2.18	Normal probability density, reproduced from [32].	42
2.19	One-tailed test, adapted from [36].	43
2.20	Two-tailed test, adapted from [36].	44
3.1	IFM and DISP obtained from the lock configuration.	47
3.2	DISP without the application of the fixator.	48
3.3	From left to right: boxplot representing DISP and E obtained in different tests with increasing thickness of Sawbones (6 mm ÷ 21.2 mm).	49
3.4	A: regression line obtained starting from the mean values of DISP for each test, B: regression line obtained starting from the mean values of E for each test. In both cases tests are done with increasing thickness of Sawbones (6 mm ÷ 21.2 mm).	50
3.5	From left to right: Sawbones to simulate the bone callus with thickness of 6 mm and 9 mm.	51
3.6	Tibial fixation with a mediolateral wire.	51

3.7	From the left to the right: IFM and DISP in the two configurations reported above with 6 mm of simulated bone callus.	52
3.8	From the left to the right: IFM and DISP in the two configurations reported above with 6 mm of simulated bone callus.	52
3.9	From the left to the right: IFM and DISP in the two configurations reported above with 9 mm of simulated bone callus.	53
3.10	From the left to the right: IFM and DISP in the two configurations reported above with 9 mm of simulated bone callus.	53
3.11	From the left to the right: IFM and DISP in the two configurations reported above with 6 mm of simulated bone callus.	54
3.12	From the left to the right: IFM and DISP in the two configurations reported above with 6 mm of simulated bone callus.	55
3.13	From the left to the right: IFM and DISP in the two configurations reported above with 9 mm of simulated bone callus.	55
3.14	From the left to the right: IFM and DISP in the two configurations reported above with 9 mm of simulated bone callus.	56
3.15	From the left to the right: IFM and DISP in the two configurations reported above with 6 mm of simulated bone callus.	56
3.16	From the left to the right: IFM and DISP in the two configurations reported above with 6 mm of simulated bone callus.	57
3.17	From the left to the right: IFM and DISP in the two configurations reported above with 9 mm of simulated bone callus.	58
3.18	From the left to the right: IFM and DISP in the two configurations reported above with 9 mm of simulated bone callus.	58
3.19	From the left to the right: IFM and DISP in the two configurations reported above with 6 mm of simulated bone callus.	59
3.20	From the left to the right: IFM and DISP in the two configurations reported above with 6 mm of simulated bone callus.	60
3.21	From the left to the right: IFM and DISP in the two configurations reported above with 9 mm of simulated bone callus.	60
3.22	From the left to the right: IFM and DISP in the two configurations reported above with 9 mm of simulated bone callus.	61
3.23	Radar plot for the ML application of the fixator. Are graphed IFM values (A) and DISP values (B) for all the configurations tested in case of simulated bone callus of 6 and 9 mm. * denotes significant difference when compared with the anatomical group.	64
3.24	Scheme of the fixator applied to the bone.	65
3.25	Radar plot for the AP application of the fixator. Are graphed IFM values (A) and DISP values (B) for all the configurations tested in case of simulated bone callus of 6 and 9 mm. * denotes significant difference when compared with the anatomical group.	66

List of Tables

3.1	6 mm simulated bone callus results.	45
3.2	9 mm simulated bone callus results.	45
3.3	Shapiro Wilk Test's p-value for 6 mm Simulated Bone Callus Data.	46
3.4	Shapiro Wilk Test's p-value for 9 mm Simulated Bone Callus Data.	46
3.5	Shapiro Wilk Test's p-value for Different Thicknesses of Simu- lated Bone Callus.	48
3.6	T-test p-values for Each Comparison	49

Bibliography

- [1] *Fractures (Broken Bones)*. URL: <https://orthoinfo.aaos.org/en/diseases--conditions/fractures-broken-bones/>.
- [2] C. S. Cánovas. “Bone elongation using monolateral external fixation: a practical guide”. In: *Strateg. Trauma Limb Reconstr.* 10.3 (Nov. 2015), pp. 175–188. DOI: 10.1007/s11751-015-0236-0.
- [3] *Limb Lengthening: The Process*. URL: <https://www.limblength.org/treatments/lengthening-deformity-correction-procedures/osteotomy/>.
- [4] *Bone structure*. URL: <https://www.fisioterapiaitalia.com/patologie/anca/fratture-del-femore/>.
- [5] *Long Bones*. URL: <https://www.humanitas.it/enciclopedia/anatomia/apparato-muscolo-scheletrico/ossa/ossa-lunghe/>.
- [6] H M Frost. “Wolff’s Law and bone’s structural adaptations to mechanical usage: an overview for clinicians.” In: *The Angle orthodontist vol. 64,3* (1994), pp. 175–188. DOI: 10.1043/0003-3219(1994)064<0175:WLABSA>2.0.CO;2.
- [7] *Callus formation and bone remodelling*. URL: <https://www.orthobullets.com/basic-science/9009/fracture-healing>.
- [8] M. Wiedemann. “Callus Distraction: A New Method?: A Historical Review of Limb Lengthening”. In: *Clin. Orthop.* 327 (June 1996), pp. 291–304. DOI: 10.1097/00003086-199606000-00036.
- [9] *Ilizarov fixator*. URL: <https://www.medicalexpo.it/prod/selaz/product-118275-810732.html>.
- [10] *TC-001T Rekrea System Manual*. URL: <https://www.citiefte.com/wp-content/uploads/2021/03/TC-001T-rev.9IT-rekrea-system-1.pdf>.
- [11] Wolfgang Roth Gernot Asche and Ludwig Schroeder. *The External Fixator. Standard indications, operating instructions and examples of frame configurations*. ISBN: 978-3887568221.
- [12] PLN Fernando et al. “An engineering review of external fixators”. In: *Medical Engineering & Physics* 98 (Dec. 2021). Epub 2021 Nov 4, pp. 91–103. DOI: 10.1016/j.medengphy.2021.11.002.

- [13] A. T. Bachmeier et al. "Novel approach to estimate distraction forces in distraction osteogenesis and application in the human lower leg". In: *J. Mech. Behav. Biomed. Mater.* 128 (Apr. 2022), p. 105133. DOI: 10.1016/j.jmbbm.2022.105133.
- [14] T. Wehner, L. Claes, and U. Simon. "Internal loads in the human tibia during gait". In: *Clin. Biomech.* 24.3 (Mar. 2009), pp. 299–302. DOI: 10.1016/j.clinbiomech.2008.12.007.
- [15] A. H. R. W. Simpson, J. L. Cunningham, and J. Kenwright. "THE FORCES WHICH DEVELOP IN THE TISSUES DURING LEG LENGTHENING. A CLINICAL STUDY". In: *J. Pediatr. Orthop.* 17.3 (May 1997), p. 416. DOI: 10.1097/01241398-199705000-00037.
- [16] Kehao Wang and Barbara Pierscionek. "Biomechanics of the human lens and accommodative system: Functional relevance to physiological states". In: *Progress in Retinal and Eye Research* (Nov. 2018). DOI: 10.1016/j.preteyeres.2018.11.004.
- [17] A STUDY OF MOMENTS ACTING ON THE TIBIA DURING GAIT IN THE ACTIVE ELDERLY POPULATION. URL: <https://ojs.ub.uni-konstanz.de/cpa/article/view/4900/>.
- [18] V. D'Angeli et al. "Load along the tibial shaft during activities of daily living". In: *J. Biomech.* 47.5 (Mar. 2014), pp. 1198–1205. DOI: 10.1016/j.jbiomech.2014.01.045.
- [19] M. Saleh et al. "Limb lengthening in congenital posteromedial bow of the tibia". In: *Strateg. Trauma Limb Reconstr.* 7.3 (Nov. 2012), pp. 147–153. DOI: 10.1007/s11751-012-0145-4.
- [20] *Mechanical and anatomical axis of long bones*. URL: <http://oldweb.unimol.it/unimolise/allegati/54074/La%20Floresta.pdf>.
- [21] *Safe Zones of the Tibia for Pin Insertion*. URL: <https://surgeryreference.aofoundation.org/orthopedic-trauma/adult-trauma/tibial-shaft/approach/safe-zones-of-the-tibia-for-pin-insertion>.
- [22] M. H. H. Ramlee et al. "Biomechanical evaluation of pin placement of external fixator in treating transverse tibia fracture: Analysis on first and second cortex of cortical bone". In: *Malays. J. Fundam. Appl. Sci.* 15.1 (Feb. 2019), pp. 75–79. DOI: 10.11113/mjfas.v15n2019.1263.
- [23] B. Narayan and N. Giotakis. "Stability with unilateral external fixation in the tibia". In: *Strateg. Trauma Limb Reconstr.* 2.1 (2007), pp. 13–20. DOI: 10.1007/s11751-007-0011-y.
- [24] A. U. Abd Aziz et al. "A finite element study: Finding the best configuration between unilateral, hybrid, and Ilizarov in terms of biomechanical point of view". In: *Injury* 51.11 (Nov. 2020), pp. 2474–2478. DOI: 10.1016/j.injury.2020.08.001.

- [25] O. Verim, M. Volkan Yaprakci, and A. Karabulut. "Biomechanical Optimization of a Novel Circular External Fixator (Optimization of Circular External Fixator)". In: *J. Med. Biol. Eng.* 37.5 (Oct. 2017), pp. 760–768. DOI: 10.1007/s40846-017-0242-4.
- [26] S. Miramini et al. "The relationship between interfragmentary movement and cell differentiation in early fracture healing under locking plate fixation". In: *Australas. Phys. Eng. Sci. Med.* 39.1 (Mar. 2016), pp. 123–133. DOI: 10.1007/s13246-015-0407-9.
- [27] M. Mühling, M. Winkler, and P. Augat. "Prediction of interfragmentary movement in fracture fixation constructs using a combination of finite element modeling and rigid body assumptions". In: *Comput. Methods Biomech. Biomed. Engin.* 24.15 (Nov. 2021), pp. 1752–1760. DOI: 10.1080/10255842.2021.1919883.
- [28] A. Martins Amaro et al. "The Effect of External Fixator Configurations on the Dynamic Compression Load: An Experimental and Numerical Study". In: *Appl. Sci.* 10.3 (2020), p. 3. DOI: 10.3390/app10010003. URL: <https://www.mdpi.com/2076-3417/10/1/3>.
- [29] P. Augat, M. Hollensteiner, and C. Von Rüden. "The role of mechanical stimulation in the enhancement of bone healing". In: *Injury* 52 (June 2021), S78–S83. DOI: 10.1016/j.injury.2020.10.009.
- [30] B. M. Hetaimish. "Sawbones laboratory in orthopedic surgical training". In: *Saudi Med. J.* 37.4 (Apr. 2016), pp. 348–353. DOI: 10.15537/smj.2016.4.13575.
- [31] C. Xu et al. "An Integrated Musculoskeletal-Finite-Element Model to Evaluate Effects of Load Carriage on the Tibia During Walking". In: *J. Biomech. Eng.* 138.10 (Oct. 2016), p. 101001. DOI: 10.1115/1.4034216.
- [32] *Normal distribution*. URL: <https://www.webtutordimatematica.it/materie/statistica-e-probabilita/distribuzioni-di-probabilita-continue/distribuzione-normale>.
- [33] S. S. Shapiro and M. B. Wilk. "An Analysis of Variance Test for Normality (Complete Samples)". In: *Biometrika* 52.3/4 (1965), pp. 591–611. ISSN: 00063444. URL: <http://www.jstor.org/stable/2333709> (visited on 11/10/2023).
- [34] George Casella and Roger L. Berger. *Properties of sufficiency and statistical tests*. ISBN: 0534243126.
- [35] T. K. Kim. "T test as a parametric statistic". In: *Korean J. Anesthesiol.* 68.6 (2015), p. 540. DOI: 10.4097/kjae.2015.68.6.540.
- [36] *T test*. URL: <https://services.ncl.ac.uk/itservice/research/dataanalysis/faqs/statisticalinferenceandsignificancetesting/>.

Acknowledgements

I deem necessary to dedicate this section of the thesis to all the people that supported me throughout my university journey and beyond.

I would like to extend my sincere appreciation to the personnel at Citieffe for hosting me and granting me the opportunity to partake in this enriching internship.

Special thanks are owed to the Technical Director, Alan Dovesi, and Fabiano Landi, whose unwavering support, valuable suggestions, and inclusion in the company made this experience truly meaningful.

I would like to thank Professor Ing. Luca Cristofolini for making this experience possible and for its guidance in the preparation of this document.

My deepest gratitude goes to my parents for their unwavering support and teachings, without which I wouldn't be who I am today. None of this would have been possible without you.

I express my thanks to my brother, despite his talent for making me angry like nobody else, I know he is the one on whom I can always count.

I want to thank my Granny, Grandpa and Marisa, for their unconditional love, for always being proud of me and for always be able to make me feel at home with a phone call.

I express my gratitude to Gio for being able to stand by me in these five years, for listening to me and for supporting me in every circumstance, for always having faith in me and for waiting from me when the exams were approaching as well as the desire for vacation.

I want to thank Bea for making herself feel close with a simple "Ciao Roccia come stai?", even though we had few opportunities to see each other in the last two years, we didn't miss a thing.

I want to thank Gio and Fede for all the moments that we were able to spend, in university or else, for instilling confidence with their words showing me the bright side and for being able to make this journey lighter and more enjoyable.

Thanks to Vitto for always being by my side, in almost all exams, for constantly supporting me, for her advices and for everything that she was able to do for me. Especial gratitude goes to her family for always welcoming me with open arms.

I want to thank Lodovica, even though we met at the end of my journey she always supported me and encouraged me in these last months.

Thanks goes also to Gaetano and Manuele for all the moments of fun and for never missing a coffee break, or an aperitif.

The time spent here has been an incredible journey, made special by every encounter, laughter with friends, lessons from professors, and the people who crossed my path. Each of you has contributed to creating unforgettable memories that I will always hold in my heart with affection and gratitude. This city has become more than just a place of study; it has become a part of me. I thank everyone for making this journey so meaningful and full of joy.

Alessandra